General Disclaimer

One or more of the Following Statements may affect this Document

- This document has been reproduced from the best copy furnished by the organizational source. It is being released in the interest of making available as much information as possible.

- This document may contain data, which exceeds the sheet parameters. It was furnished in this condition by the organizational source and is the best copy available.

- This document may contain tone-on-tone or color graphs, charts and/or pictures, which have been reproduced in black and white.

- This document is paginated as submitted by the original source.

- Portions of this document are not fully legible due to the historical nature of some of the material. However, it is the best reproduction available from the original submission.

LINE BLANKETING IN VEGA AND SIRIUS

Grant NSG 5030

Final Report

Principal Investigator
Dr. Robert L. Kurucz

Prepared for

National Aeronautics and Space Administration
Goddard Space Flight Center
Greenbelt, Maryland 20771

Smithsonian Institution
Astrophysical Observatory
Cambridge, Massachusetts 02138

The Smithsonian Astrophysical Observatory
and the Harvard College Observatory
are members of the
Center for Astrophysics

The NASA Technical Officer for this grant is Dr. James E. Kupperian, Code 410, OAO Projects, Projects Directorate, Goddard Space Flight Center, Greenbelt, Maryland 20771.

LINE BLANKETING IN VEGA AND SIRIUS

Grant NSG 5030

Final Report

Principal Investigator
Dr. Robert L. Kurucz

Prepared for
National Aeronautics and Space Administration
Goddard Space Flight Center
Greenbelt, Maryland 20771

Smithsonian Institution
Astrophysical Observatory
Cambridge, Massachusetts 02138

The Smithsonian Astrophysical Observatory
and the Harvard College Observatory
are members of the
Center for Astrophysics

The NASA Technical Officer for this grant is Dr. James E. Kupperian, Code 410, OAO Projects, Projects Directorate, Goddard Space Flight Center, Greenbelt, Maryland 20771.

TABLE OF CONTENTS

ABSTRACT

Our theoretical model and spectrum calculation for Vega seem to be realistic once we have corrected a few errors in the Kurucz and Peytremann line list. The abundance of carbon is approximately -3.8, which is 0.3 lower than the old solar value and supports Mount and Linsky's newer value. The oxygen abundance is approximately -3.5. Assuming that Vega has solar abundances, the solar oxygen abundance appears to have been overestimated by 0.3 in the log. Other abundances appear to be solar.

For Sirius the calculations do not agree with the observed spectrum. Line opacity is considerably underestimated, notably in third-spectrum iron group lines. Carbon is underabundant relative to Vega by 0.2 in the log. Nitrogen is unchanged. Oxygen is enhanced by 0.3. Heavier elements are enhanced by 1.0 in the log.

Our tentative calibration yields 1.3E-10 ergs/cm^2/s/nm for each U1 Copernicus count at 130 nm.

LINE BLANKETING IN VEGA AND SIRIUS

Final Report

1. INTRODUCTION

Vega and Sirius are two of the brightest, best observed stars. Vega is the archetypical "normal" star that we would expect to have solar or, because it was formed more recently than the sun, slightly enhanced solar abundances. Its angular diameter and distance are known and it does not suffer from theoretical problems such as convection, so one should be able to calculate realistic theoretical models and spectra. For any model atmosphere program or spectral calculation program to be considered accurate and realistic it must reproduce, at least in a general way, the spectrum and energy distribution of Vega. Furthermore, because photometric systems ultimately are defined relative to Vega, theoretical interpretation of photometry depends on the calculation of a model for Vega.

Once theoretical programs are available to treat normal stars, simple parameter changes should allow the prediction of models for evolved stars and stars of different populations. Sirius is a moderately metallic line star, a binary with a white dwarf companion that presumably transferred matter enriched in heavy elements to Sirius A. The mass, diameter, and distance are known for Sirius, and, because it is easily observed at high resolution, it makes a good test case for checking the effects of abundance changes.

With theoretical programs for computing models and spectra, we are investigating Vega and Sirius over the whole spectral range both to determine the properties of the stars themselves and to test the programs. Copernicus provides a unique opportunity to obtain spectra that show strong resonance lines of many elements and many other lines formed through a range of levels in the atmosphere. Such spectra present a strong test of the stellar atmosphere theory.

2. COPERNICUS OBSERVATIONS

Copernicus U1 scans of Vega and Sirius were made during September and November 1974 covering the region 130 to 135 nm with a resolution of approximately 0.0037 nm. We went to Princeton in December 1974 to collect the data.

In Figure 1 we show the scans for both stars normalized as discussed in Section 10. The individual data points for Vega are visible in Figure 8 and for Sirius in Figure 9. Since full scale at 130 nm corresponds to 2400 counts for Sirius and only 575 for Vega, the Vega scan is considerably noisier. The scans were made in small overlapping sections but one piece at 132.9 was not observed in Sirius. The Sirius wavelengths have been incremented by 0.003 nm to align the two spectra approximately, but no other effort has been made to process the data. Wavelengths should be considered uncertain by at least this amount. Although the noise causes some uncertainty, it appears that the same features appear in both spectra, that the stronger features are of similar strength in both stars (e.g., O I at 130.2 and C I at 132.9), but that many features weak in Vega are tremendously increased in Sirius.

3. MODEL ATMOSPHERE FOR VEGA

Observations are available for Vega in the visible that allow a reasonably accurate determination of model parameters. A good fit in the visible is important to this analysis because the far ultraviolet falls on the exponential side of the Planck maximum and, thus, is sensitive to small temperature changes. Conversely, the far ultraviolet continuum and line spectrum provide strong tests of the models because they are so sensitive.

We have computed a grid of model atmospheres that include line opacity in the form of statistical distribution functions (Kurucz, in preparation). By comparing these models to the energy distribution determined by Hayes and Latham (1975) we determined parameters $T_{eff} = 9400 \pm 200$ K and $\log g = 4.0 \pm 0.5$. Then, with Deane Peterson at Stony Brook, we programed the Vidal, Cooper, Smith theory (Vidal, Cooper, and Smith, 1973) for hydrogen line profiles. By comparing to Peterson's (1969) Balmer line profiles we determined $\log g = 3.95 \pm 0.05$. These parameters are consistent with Code's (1975) empirical values, 9660 ± 130, and 3.94 ± 0.08. Figures 2 and 3 show the comparisons between the observations and a 9400, 3.95 model. There is a small discrepancy in that the Balmer line cores are narrower than those observed. As discussed in Section 7, Vega has a projected rotational velocity of approximately 25 km/s. Rotationally broadening the theoretical profile would widen the core to match but would leave the central residual intensity too high. Non-LTE effects, which have not been included, presumably would lower the central intensity (Peterson, 1969).

This model was computed assuming solar abundances from Withbroe's compilation (1971). Thus we assumed -3.48 for the log carbon abundance relative to the total. However, as discussed in Section 9, the actual carbon abundance is nearer -3.8. Since the carbon continua are important features in the far ultraviolet, the abundance change reduces the total ultraviolet opacity and decreases the backwarming. This may mean that a slightly hotter model with the new abundances may be more correct. We have not yet determined the magnitude of such a correction.

4. MODEL ATMOSPHERE FOR SIRIUS

In the grid calculation described above, it is a simple matter to compute models at scaled solar abundances, but it is expensive to make changes that require recomputing line opacity. As a moderately metallic line star, Sirius has decidedly nonscaled abundances, with light elements near solar and with metals overabundant by a factor of 10 or so (Kohl, 1964; Latham, 1970). As a first step we tried the approximation of a 10,000,4.3 model with all abundances increased by 0.5 in the log. These parameters are approximately Code's (1975), 9975 ± 150 and 4.31 ± 0.04. This model agrees fairly well with Peterson's (1969) Balmer line profiles and with the energy distribution given by Latham (1970), corrected to the new calibration of Vega by Hayes and Latham (1975). It would be useful to have new, improved observations of the energy distribution of Sirius.

The initial spectrum calculation with abundances increased by 0.5 in the log was grossly inconsistent with the observations. We were able to improve the fit by changing abundances of various elements. Then we computed a model with abundances C -4.00, N -4.00, O -3.22, and heavier elements 10 times solar, but with line opacity tables computed for abundances 10 times solar. Thus the model is not consistent. We are currently using this model in the spectrum calculations; but, as discussed in Section 9, there remain inconsistencies in the spectrum indicating that the model may need improvement.

5. SPECTRUM SYNTHESIS PROGRAM

We have continually improved our spectrum synthesis program during the course of this research. The basic program works as follows. For a given model atmosphere tabulated at 40 depths, we compute number densities and partition functions for all atoms and ions. Then we read the magnetic tape that lists the gf values calculated by Kurucz and Peytremann (1975, hereinafter called KP) and compute a line opacity spectrum at each depth. The expressions for radiative, Stark, and van der Waals broadening are

$$\Gamma_R = \Gamma_{classical} = 2.223E13/\lambda^2 \quad , \qquad \lambda \text{ wavelength in nm} \quad ;$$

$$\Gamma_S = 1.0E\text{-}8\ n_{eff}^{\ 5}\ N_e \quad ;$$

$$\Gamma_W = 4.5E\text{-}9\ \langle r^2 \rangle^{4/10}\ [N_H + 0.42\ N_{He} + 0.85\ N_{H_2}]\ (T/10,000)^{3/10} \quad ;$$

where

$$\langle r^2 \rangle = 2.5\ n_{eff}^{\ 2}/Z_{eff}^{\ 2} \quad ,$$

$$n_{eff}^{\ 2} = R\ Z_{eff}^{\ 2}/E_{up} \quad ,$$

Z_{eff} is the charge plus 1, E_{up} is the upper level energy, and R is the Rydberg energy. Next, continuum quantities, opacities, source functions, and fluxes, are evaluated at several points in the wavelength interval. Then, the continuum quantities are interpolated to each point in the spectrum, the line opacity added, the source function approximated by

$$[(\kappa + \sigma)S_{cont} + \ell\ S_{line}]/(\kappa + \sigma + \ell) \quad ,$$

and the surface flux or intensity computed. Here κ and σ are the continuous absorption and scattering coefficients, ℓ is the line absorption coefficient, S_{cont} is the continuum source function, and S_{line} is the line source function, which is assumed to be the Planck function.

The following improvements have been made. We have computed mean square radii for the 4p orbitals of the iron group atoms and ions, and produced an interpolation formula

$$\langle r^2 \rangle = (45 - A + Z)/(Z + 1) \quad ,$$

where A is the atomic number and Z is the charge. This expression is used for van der Waals broadening of all iron group atoms, assuming that the strong lines are all resonance lines with a 4p upper state.

There is now provision for additions, deletions, and corrections to the table of gf values and for use of individual "real" radiative, Stark, and van der Waals damping constants for each line.

To resolve the contribution of individual lines to blends, we now compute, in addition to the spectrum, the central intensity for each line in isolation.

We automatically produce spectrum plots with identifications.

6. ROTATIONAL BROADENING OF THE THEORETICAL SPECTRUM

In practice, most spectra must be rotationally broadened to compare with observations. We have developed a broadening procedure of direct numerical integration over the stellar disk. This procedure is simple and easily generalized to treat gravity darkening, nonuniform rotation, nonspherical stars, and binaries. In the simple case of uniform rotation, no gravity darkening, and circular projection, we can use symmetry to reduce the evaluation to one quadrant.

The integration is performed by laying a grid of any fineness over the stellar disk and simply adding the intensity at each point. For the calculations reported here we used a spacing of 0.02 times the radius. At each point on the grid we compute the doppler shift and the cosine of the angle of projection. The doppler shift is converted to an integral number of steps in the spectrum (multiples of the point spacing) and the cosine is converted to an integral multiple of 0.01. In general there will be grid points on the disk that have the same values of these integers. All the values are sorted and the multiplicity of each is noted. The multiplicities are added and a normalization factor is determined such that integration of I_ν produces H_ν. This set of numbers is the rotation operator.

For the work described here we computed the spectrum with a spacing of 0.5 pm at 17 angles and interpolated to 100 cosines from 0.005 to 0.995. These spacings were chosen arbitrarily. Smaller spacings might improve the accuracy of the final spectrum. Fewer angles than 17 are possible. We should point out that computation time is not proportional to the number of angles since the opacity spectrum need be computed only once for any number of angles.

To broaden the spectrum rotationally, we read the intensities $I_{j\mu}$ one wavelength at a time and distribute each intensity into a flux spectrum H using the rotation operator. For example, if part of the operator is an 11-step doppler shift for a cosine index μ of 37 with a multiplicity of 4, we would add $4I_{j37}$ to H_{j+11} and, by

symmetry, to H_{j-11}. Thus we go through every term of the operator for every wavelength in the spectrum. Once the totals are completed we normalize. If the doppler width of the operator includes many steps, N, the accuracy is improved by filtering with a (1 + N/5)-step straight mean. The accuracy of this procedure is better than 1 percent for computing flux from intensity at zero rotation velocity, for the parameters quoted. The accuracy can be improved to any desired limit by increasing the resolution.

7. ROTATION OF VEGA AND SIRIUS

These stars have quite significant projected rotational velocities that blend the lines and greatly complicate the analysis. We have been collaborating with Ingemar Furenlid at Kitt Peak and with John Lester at SAO to obtain high-resolution, low-noise spectra in the visible. Through visual examination of 1 A/nm plates taken by Furenlid, we estimate velocities of 15 to 20 km/s for Sirius and 25 to 30 km/s for Vega. These spectra have not yet been reduced so we have assumed velocities of 15 and 25 km/s in our calculations thus far. The zero velocity and rotationally broadened spectrum for Vega is shown in Figure 4 and for Sirius in Figure 5. The observed Copernicus spectra suggest a velocity somewhat larger than 15 km/s for Sirius and seem consistent with 25 km/s for Vega.

We have also undertaken a project with Wesley Traub, Nathaniel Carleton, and John Lester of SAO to measure a Ba II line profile in Sirius with a high-resolution interferometer. Since the project was begun before we found that Sirius has a high rotation velocity, we had hoped to determine both a rotation velocity and a maximum turbulent velocity. The reductions have not yet been completed, but we provisionally find a rotation velocity of 17 km/s.

8. THEORETICAL LINE LIST

One of the aims of this research is to check the available line data for accuracy and completeness and to identify areas where further work is required. Our basic source of these data is the KP line list, which was computed, for sequences up through nickel, by using scaled Thomas-Fermi-Dirac wavefunctions and eigenvectors found through least-squares fits of eigenvalues to observed levels (Kurucz, 1973). Heavier elements and the lightest elements were taken from the literature. The data published by KP represent only a fraction of the lines calculated, those between known levels. There are many lines between predicted levels that cannot be used for spectrum synthesis because the wavelengths are uncertain, but which can be used in computing the statistical distribution functions for the model atmosphere calculations.

We emphasize that spectroscopic analyses of many elements leave considerable room for improvement. There are levels that have not been classified, and so cannot be included in a gf calculation, and there are levels that are misclassified. Most important, many analyses are highly incomplete. Several of the iron group second spectra have not even been observed in the vacuum ultraviolet. We expect such lines account for a number of unidentified features in the Copernicus spectra.

Through examination of Kelly and Palumbo's (1973) line list and the ultraviolet multiplet table (Moore, 1962) we have found one prominent example of the incompleteness of KP. Multiplet 56 of Mn II is not in the list because the upper term has not been classified and so could not be computed. Kelly and Palumbo list a number of weak lines that have not been classified and do not appear in KP.

Thus far we have identified two sorts of errors in the KP line list through the presence of identifiable observed lines where the line list predicts none, and through the presence of a prominent predicted feature where none is observed. Several C II, N III, and Si II transitions involving sp^2, and several O I, Si II, and S I transitions involving an excited parent, are missing, presumably through programing mistakes. These errors may also occur in other elements that have not yet been checked.

Fortunately, these strong lines appear in the NBS compilations (Wiese, Smith, and Glennon, 1966; Wiese, Smith, and Miles, 1969; Wiese and Glennon, 1972). We have also found a few excited, LS forbidden, C I and N I lines that are computed too strong. Apparently the eigenvector mixing was overestimated.

In general, we assume that laboratory gf values based upon lifetime measurements are more reliable than KP. We are undertaking to replace KP data with such data, especially from the NBS compilations. However, we expect KP to be more accurate than NBS coulomb approximation f values and to give better relative strengths within multiplets than NBS LS multiplets.

We are also undertaking to include radiative and Stark damping constants for the stronger lines. At the present time we are filling in transition arrays and summing A's by hand to get the radiative damping constants. Programs are under development that will produce the radiative damping constants for every transition of an element. The sources used thus far for Stark broadening are Sahal-Brechot and Segre (1971) and Griem (1974). To use Griem's widths we compute

$$\Gamma_s/N_e = 3767\ W/\lambda^2$$

with width W at 10,000 or 20,000 K and wavelength λ in A. We have not yet included all Griem's data.

We expect to publish, either as part of this work, or as a separate publication, tables of these revisions.

9. COMPARISON OF THE SPECTRA

Figures 6 and 7 show the current theoretical and observed spectra for Vega and Sirius normalized as discussed in Section 10. Figures 8 and 9 are the same plots with identifications for all theoretical lines with zero rotation residual fluxes less than 0.99 in Vega and 0.98 in Sirius. In calculating the spectra the 9400, 3.95 and 10,000,4.3 models described in Sections 3 and 4 were used. In Vega the carbon abundance with reduced from -3.48 to -3.8. A microturbulent velocity of 2 km/s was assumed for the time being.

Since improvements and corrections to the program and line data are an ongoing process, the current plots are the result of a long series of iterations. Except for the abundance changes described in Sections 3 and 4 and below, no attempts have been made to adjust individual lines for a match. The fit is remarkably good for Vega. For Sirius a number of lines match very well but the majority of the lines are grossly underestimated in the calculations. No fourth spectrum or higher lines appear in either the calculations or the observations. In the discussion of individual elements below we assume that the gf values and damping constants are correct. (We use the terms weak and strong to refer to the comparison, calculation relative to observation, not to the strengths of the lines.)

Hydrogen. There is background Lyman α wing but the Vega data are too noisy and the match in Sirius is not good enough to draw any conclusions at this time.

Helium, Lithium, Beryllium, Boron. There are no lines in this spectral region.

Carbon. The C I resonance lines at 132.9 are computed too strong in Vega but match well in Sirius. The lines around 131.1 from the ^{1}D lower level are blended in features that are calculated too weak. The continuum in this region arises from the ^{1}S level. The C II resonance lines at 133.5 are computed with approximately correct cores. The wings are not right in Vega but there may be lines present in

the noise. A C III line at 130.870 does not appear in the spectra. Since C is mainly C II we would expect the C II lines to be more reliable abundance indicators, and the C I lines to be much more sensitive to atmospheric variations. For abundances other than -3.8 in Vega and -4.0 in Sirius the C II lines are discrepant.

Through personal conversations with M. A. J. Snijders of Goddard, we found that his non-LTE calculations predict increased ionization of C I in Vega and LTE in Sirius. Thus the C I lines would become weaker in Vega without significantly changing the C II lines. The strength of the continuum would also be reduced.

Since we expect Vega to have solar abundances, the solar abundance of C may be overestimated by a factor of 2. Such a result has been found by Mount and Linsky (1975) through analysis of solar molecular features. Sirius is depleted in C by 0.2 in the log relative to Vega.

Nitrogen. There is an isolated N I doublet at 131.967 that is a good match. The blended features at 131.89 and 130.00 are difficult to interpret. N II lines at 134.3, 134.5, and 134.6 do not appear in the predicted spectra, but there are features in the observed spectra. N III lines do not appear. The N abundance is equal and approximately solar in both stars.

Oxygen. The O I resonance lines at 130.2, 130.4, and 130.6 are predicted too strong in Vega and approximately correct in Sirius. We have not yet determined the O abundance in Vega but we guess -3.5. Since we expect Vega to have solar abundances, we suggest that the solar abundance should be -3.5 instead of -3.22, which is currently assumed. In Sirius the abundance is approximately -3.22, a factor of 2 enhanced over Vega.

Fluorine. There are no F I lines in this region. The high excitation F II lines at 132.7, 132.8, 133.2, 133.3, 134.3, and 134.4 do not appear in the calculations, however, in some cases, observed features do correspond. The same situation applies to F III. We can say nothing about the F abundance.

Neon. There are no Ne lines in this region.

Sodium. There are no Na I lines in this region. Na II and III lines do not appear in either spectrum.

Magnesium. There are no Mg I lines in this region. In Vega, the Mg II lines match at 130.67 and 130.82, are too strong at 130.78, and are blended at 130.94. In Sirius, 130.67 matches while 130.78 and 130.82 are slightly strong. Mg III lines do not appear. The Mg abundance is approximately solar in Vega and +1.0 in Sirius.

Aluminum. There are no Al lines in this region.

Silicon. There are no Si I lines in this region.

Si II: 130.08 weak
130.43 blend, strong
130.56 blend, good
130.9 blend, good
134.68 Vega, slightly strong; Sirius, strong
134,85 Vega, slightly strong; Sirius, strong
135.0 strong

Si III: 130.11 slightly strong
130.33 blend, strong
131.25 weak?
134.24 blend
134.33 blend

The Si abundance in Vega is approximately solar and in Sirius at least +1.0. The models predict the correct ionization.

Phosphorus. The P I line at 130.447 is blended. P II lines at 130.18, 130.46, 130.54, 130.98, and 131.07 are blended in such a way that one can tell the lines are approximately the right strength. Of the P III lines, 133.48 is blended and, in Sirius, blended and strong, 134.43 is blended and strong, 134.49 possibly matches. The wavelengths are discrepant. Other lines do not appear in either star. The P abundance is approximately solar in Vega and +1.0 in Sirius. The models predict the correct ionization.

Sulfur.

S I:
- 130.23 blend
- 130.28 blend, slightly strong
- 130.31 blend, slightly strong
- 130.34 blend, slightly strong
- 130.58 blend, good
- 131.01 blend, good
- 131.32 blend, good
- 131.65 slightly strong
- 132.35 slightly strong
- 132.66 blend, slightly strong
- 133.37 blend, strong

There are no S II lines in this region. S III lines do not appear in the spectra. The sulfur abundance is approximately solar in Vega and +1.0 in Sirius.

Chlorine. The Cl I line at 133.57 is blended. The line at 134.72 is slightly weak. There are no Cl II or III lines in this region. The Cl abundance is approximately solar in Vega and +1.0 in Sirius.

Argon. There are no Ar I lines in this region. There is an Ar II line at 134.72 that does not appear in the predicted spectrum for Vega but does weakly in the predicted spectrum for Sirius. There is an observed feature in both stars at this wavelength that is stronger in Sirius. These lines are highly excited and would be very sensitive to temperature changes. There are no Ar III lines in this region. We can draw no conclusions about the abundance of Ar.

Potassium. There are no K lines in this region.

Calcium. There are no Ca I lines in this region.

Ca II:
- 130.56 masked
- 132.98 blended, strong in both stars
- 133.09 match in both
- 134.18 slightly weak in both
- 134.25 blend, slightly weak in Vega, matches in Sirius

Ca III lines do not appear in the predicted spectra. There is an unidentified feature at 133.74, which is the wavelength of one of the lines. The Ca abundance is approximately solar in Vega and +1.0 in Sirius.

Scandium. There are no Sc I or III lines in this region. Sc II lines have not yet been observed in this region.

Titanium. There are no Ti I lines in this region. Ti II lines have not yet been observed in this region. Ti III 132.75 matches in both stars, 132.98 is blended, and 133.96 is noisy in Vega and matches in Sirius. The Ti abundance is approximately solar in Vega and +1.0 in Sirius.

Vanadium. There are no V I lines in this region. There are six V II lines that are masked, blended, or insignificant. A feature is observed in Sirius at 131.38, but the calculated feature is much weaker. There are a dozen V III lines but they are all masked, blended, or insignificant. We can say nothing about the V abundance.

Chromium. There is no Cr I in this region. Cr II has not yet been observed. The relative strengths of Cr III lines are the same in both stars but many of the lines are very noisy in Vega.

Cr III:	131.15 blended, masked	132.16 blend, weak
	131.40 very weak	132.28 weak
	131.54 masked	132.84 very weak
	131.64 blend, slightly strong	133.15 blend, weak
	132.00 very weak	133.77 weak

Either Cr has a greatly enhanced abundance or there is some error in the models that produces the wrong ionization for Cr III.

Manganese. There are no Mn I lines in this region.

Mn II: 130.10 blend, strong in both stars
130.67 blend
133.15 blend, weak
134.43 blend, strong
134.56 weak

The gf values for multiplet 56 could not be computed by KP but the lines are present in the observed spectra,

130.56 masked
131.34 masked
131.37 present in both stars, stronger in Sirius
131.73 may be present in blend
131.77 present in Sirius, not apparent in Vega
131.80 present in both stars, stronger in Sirius.

The Mn III line at 134.76 is very weak. We can draw no conclusions about the Mn abundance.

Iron. There are no Fe I lines in this region. There are numerous Fe II and Fe III lines. We get the impression that many features observed in Sirius correspond to Fe III lines that are weak in the calculated spectrum. It is possible that this is a coincidence because there are so many lines. In Vega, the noisiness and questions about the normalization level make the comparison difficult for many of the weaker features. In Vega there are a number of Fe II lines that seem to match so we guess that the abundance is approximately solar. In Sirius those lines are predicted slightly weak which may indicate an Fe abundance increase greater than 1.0. There seem to be problems with ionization and Boltzman factors.

Cobalt. There are no Co I lines in this region. The Co II lines at 130.69, 131.18, and 131.81 are weak in both stars. Other lines are masked or blended. The Co III line 132.68 is not seen in Vega and is predicted to be insignificant in Sirius. The Co abundance is greater than solar in Vega and greater than +1.0 in Sirius. The solar Co abundance may be underestimated.

Nickel. There are no Ni I lines in this region. There are numerous Ni II lines. The resonance lines at 130.88, 131.72, 133.52, and 134.58 match. Higher excitation lines are weak but correspond to many features. The Ni III lines are weak. There seems to be some ionization problem. If some way could be found to increase the strength of the weak Ni II and III lines the calculated spectra would fit much better.

Copper. There are no Cu I lines in this region. Cu II lines do not appear in Vega. Two lines, 130.39 and 133.18, are predicted as small in Sirius. No Cu III lines appear in any of the spectra.

Zinc. Zn I lines have not been observed in this region. The Zn II line at 130.6741 was not computed by KP but may be present in the observed spectra. All Zn III lines are insignificant or masked.

Elements heavier than the nickel sequence. Heavier elements were not computed by KP and gf values for lines in this region were not available from the literature so the line list does not predict any heavy lines in this region. An examination of Kelly and Palumbo (1973) and Moore (1962) does not produce any obvious identifications. Detailed searches will be made in the future.

Our overall impression is that there is a temperature problem with the models because resonance lines of lighter elements seem to match in all stages of ionization, while highly excited iron group lines are predicted too weak. Further work is required to determine whether temperature increases will resolve the discrepancy. Temperature changes in Vega cannot be very large because of the good fits with the strong lines and in the visible.

10. CALIBRATION OF COPERNICUS IN THE REGION 130 TO 135 nm

We have assumed that the wavelength dependence of the Copernicus sensitivity did not vary in the time between the observations of the two stars so the same relative shape applies to both Sirius and Vega. In plotting the spectra we overlaid the observations on the calculations and determined a relative shape and the number of counts at full scale required to force a match. Currently, the counts are 2400 for Sirius and 575 for Vega at 130 nm. The shape factor that converts from counts to energy is given in this table:

Wavelength	130 nm	131	132	133	134	135
Factor	1	1.0	1.0	1.1	1.1	1.2

The noisiness of the Vega spectrum and the large number of lines in the Sirius spectrum that do not match leave considerable room for subjective fitting. Since there are several places in Vega where the observed spectrum rises above the calculated spectrum, these numbers will probably be revised.

To determine the absolute calibration in ergs/cm^2/s/nm per count in U1, we use the angular diameters measured by Hanbury Brown, Davis, and Allen (1974). The flux at the earth is inversely proportional to the square of the distance,

$$\text{flux} = (R_*/D)^2\, 4\pi H_\lambda = (\theta/2/206265)^2\, 4\pi H_\lambda \quad ,$$

where θ is the angular diameter of the star in arc seconds. At 130 nm we find

	Sirius	Vega
θ	0.00589 ± 16	0.00324 ± 7 arc sec
H_λ, full scale	1.320E8	8.842E7 ergs/cm^2/s/ster/nm
U1 counts, full scale	2400	575
flux/count	1.41E-10	1.20E-10 ergs/cm^2/s/nm/count

11. FURTHER WORK

We expect to compute one or two more iterations of the Vega spectrum to determine the oxygen abundance and include additional damping constants. We also plan to check for non-LTE effects in C I using b's computed by Snijders and another spectrum synthesis program that we have developed to do non-LTE spectra. We need to make another iteration on Sirius with the additional damping constants and we will attempt to identify additional features. This additional research and this final report will be submitted to the Astrophysical Journal Supplement.

We will apply for additional observing time on Copernicus to obtain as much of the spectra of the two stars as possible, hopefully with lower noise in Vega. In fact, we believe that observations of Sirius and Vega are so important that Copernicus should be used to produce atlases for the two stars.

Since we are undertaking a detailed analysis of both stars in the visible as well as the ultraviolet, we think that detailed discussion of f values and individual abundances should wait until complementing observations from all spectral regions can be considered together.

12. REFERENCES

CODE, A. D.

1975. Empirical effective temperature, bolometric corrections, and fundamental stellar properties. Proceedings of a Conference, Multicolor Photometry and the Theoretical HR Diagram. Dudley Obs. Rep. No. 9, ed. by A. G. Davis Philip and D. S. Hayes, pp. 221-240.

GRIEM, H. R.

1974. Spectral Line Broadening by Plasmas, Academic Press, New York, 408 pp.

HANBURY BROWN, R., DAVIS, J., and ALLEN, L. R.

1974. The angular diameters of 32 stars. M.N.R.A.S., vol. 167, p. 121.

HAYES, D., and LATHAM, D.

1975. Astrophys. Journ., vol. 197, p. 593.

KELLY, R. L., and PALUMBO, L. J.

1973. Atomic Emission Lines below 2000 Angstroms. U.S. Naval Research Lab., Washington, 992 pp.

KOHL, K.

1964. Die Atmosphäre des Sirius. Zs. f. Ap., vol. 60, p. 115.

KURUCZ, R. L.

1973. Semiempirical calculation of gf values: Sc II $(3d+4s)^2$ - (3d+4s) 4p, a detailed example. Smithsonian Astrophysical Obs. Spec. Rep. No. 351, 57 pp.

KURUCZ, R., and PEYTREMANN, E.

1975. A table of semiempirical gf values. Smithsonian Astrophysical Obs. Spec. Rep. No. 362.

LATHAM, D. W.

1970. Abundances of the elements in Sirius and Merak. Smithsonian Astrophysical Obs. Spec. Rep. No. 293.

MOORE, C. E.

1962. An ultraviolet multiplet table, U.S. National Bureau of Standards, Circ. 488, Sec. 4, 65 pp; Sec. 5, 30 pp.

MOUNT, G. H., and LINSKY, J. L.

1975. A new solar carbon abundance based on non-LTE CN molecular spectra. Astrophys. Journ., vol. 202, p. L51.

PETERSON, D. M.

1969. Balmer lines in early type stars. Smithsonian Astrophysical Obs. Spec. Rep. No. 293.

SAHAL-BRÉCHOT, S., and SEGRÉ, E.

1971. Semi-classical calculations of electron and ion collisional broadening of the strongest U. V. ionic lines of astrophysical interest. Astron. Astrophys., vol. 13, pp. 161-168.

VIDAL, C. R., COOPER, J., and SMITH, E. W.

1973. Hydrogen Stark-broadening tables. Astrophys. Journ. Suppl., vol. 25, p. 37.

WIESE, W. L., and GLENNON, B. M.

1972. Section "Atomic Transition Probabilities," in American Institute of Physics Handbook. McGraw-Hill Book Co., New York, pp. 7-200 to 7-263.

WIESE, W. L., SMITH, M. W., and GLENNON, B. M.

1966. Atomic Transition Probabilities. Vol. I. Hydrogen through Neon. National Standard Reference Data Series, Nat. Bur. Stand., vol. 4, 153 pp.

WIESE, W. L., SMITH, M. W., and MILES, B. M.

1969. Atomic Transition Probabilities. Vol. II. Sodium through Calcium. National Standard Reference Data Series, Nat. Bur. Stand., vol. 22, 306 pp.

WITHBROE, G. L.

1971. The chemical composition of the photosphere and the corona. In The Menzel Symposium Solar Physics, Atomic Spectra, and Gaseous Nebulae, ed. by K. B. Gebbie, Nat. Bur. Standards Spec. Publ. 353, pp. 127-148.

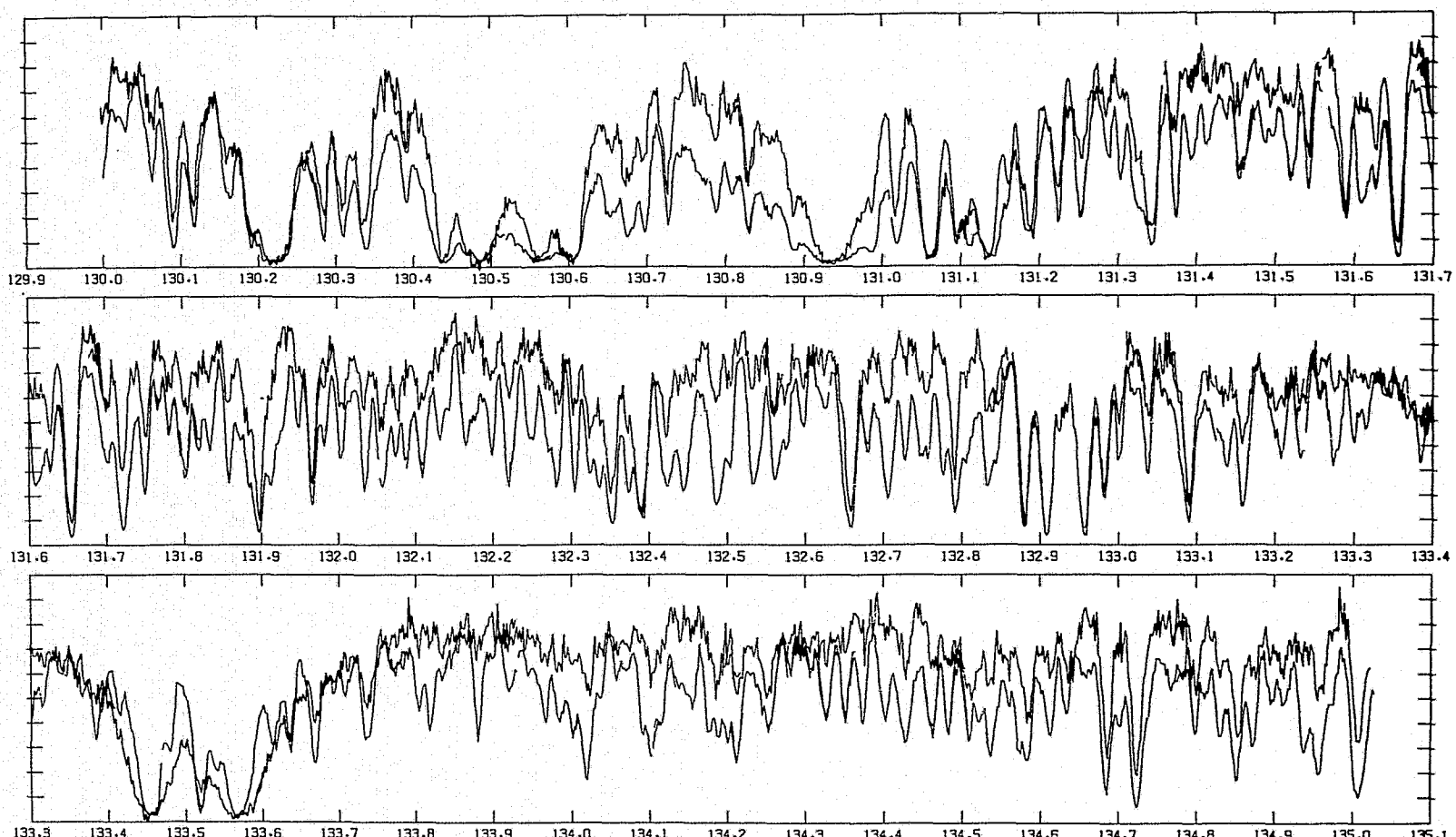

Figure 1. Copernicus Ul spectra of Vega and Sirius for the interval 130 to 135 nm. Sirius is the less noisy, generally lower curve. Full scale at 130 nm corresponds to 2400 counts for Sirius and 575 for Vega. Figures 8 and 9 show the individual data points.

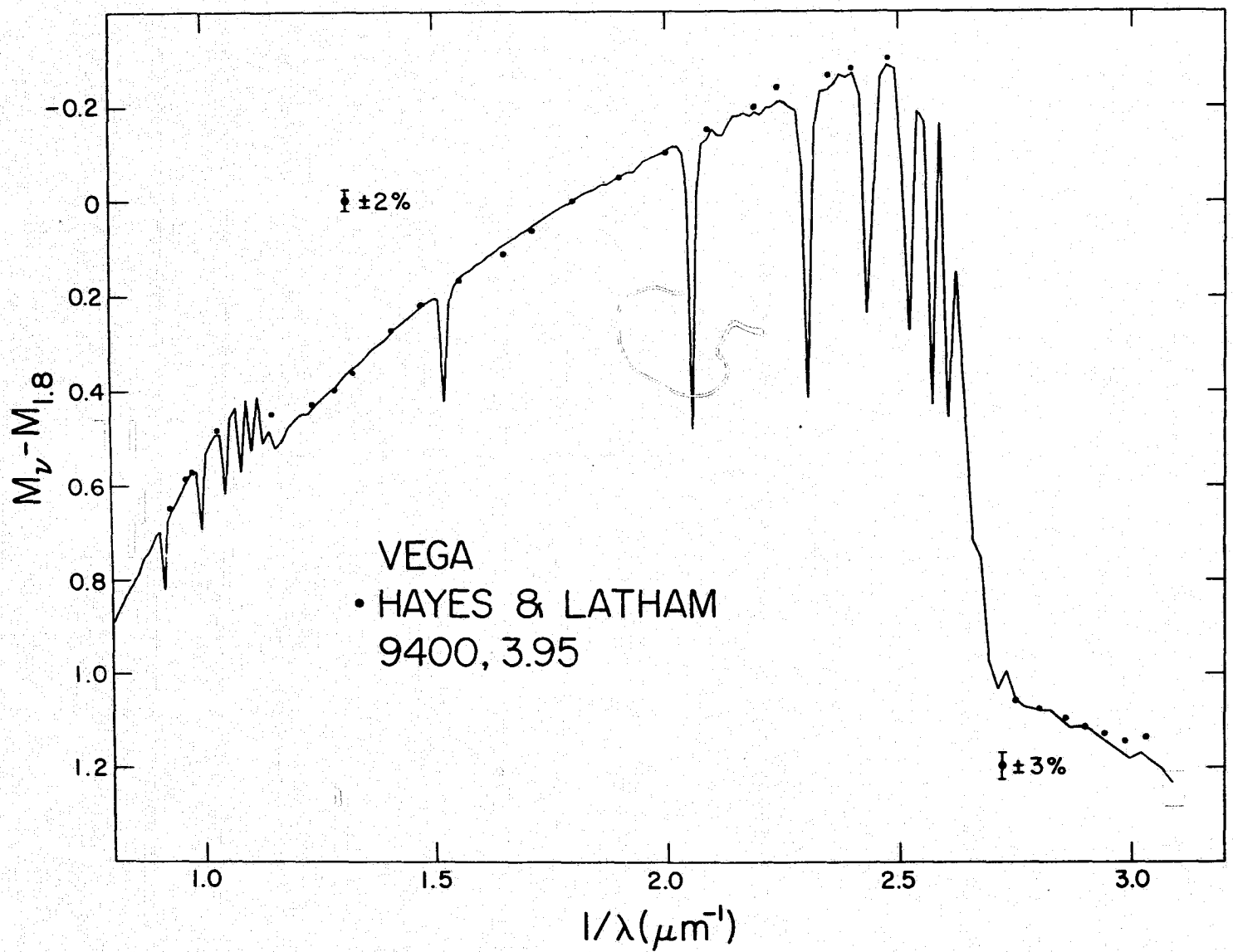

Figure 2. Comparison of the colors of the theoretical model with $T_{eff} = 9400$, $\log g = 3.95$ with the new Vega observations of Hayes and Latham (1975). Error bars for the observations are indicated.

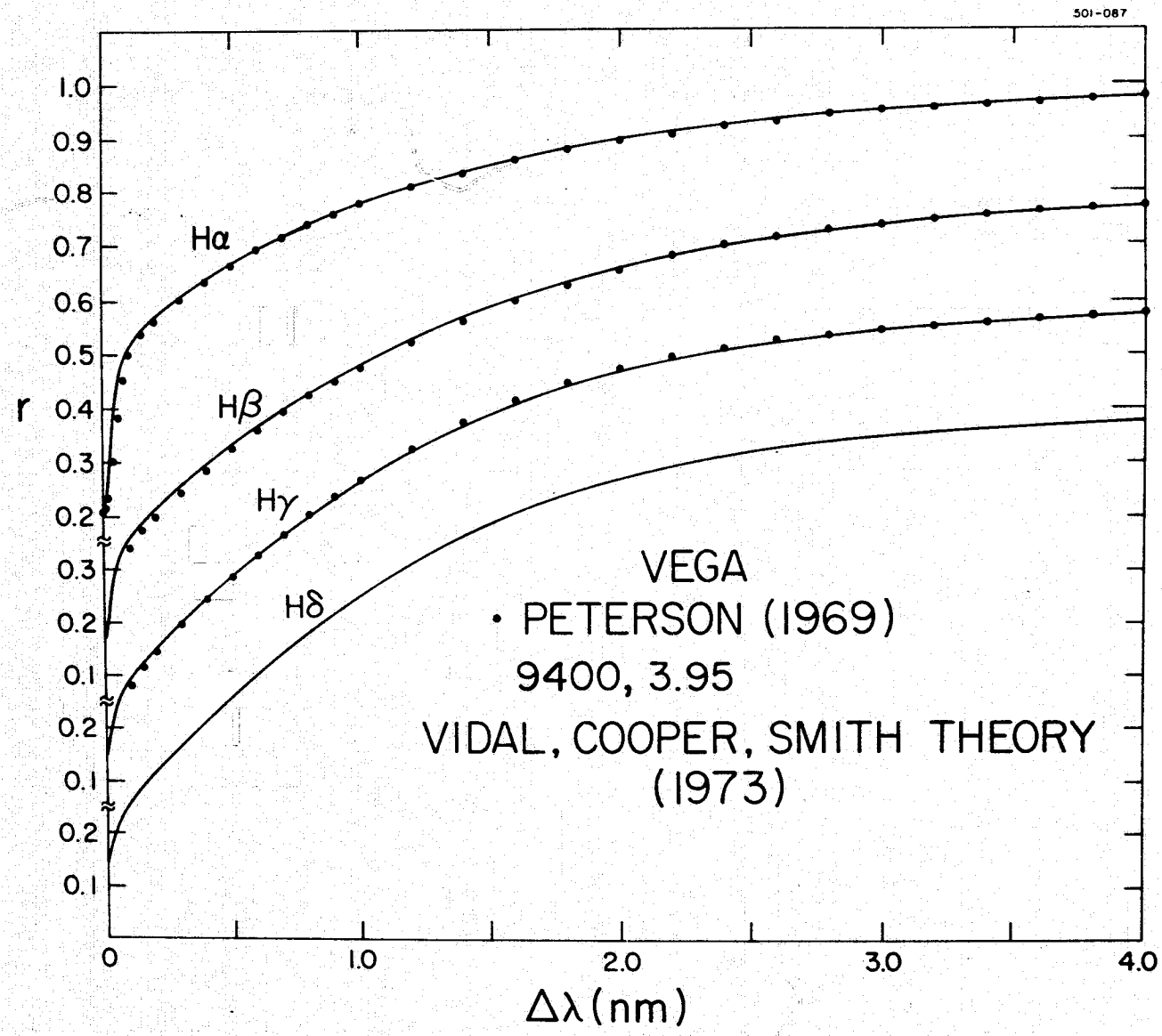

Figure 3. Theoretical Balmer line profiles for the same model compared with the observations of Peterson (1969).

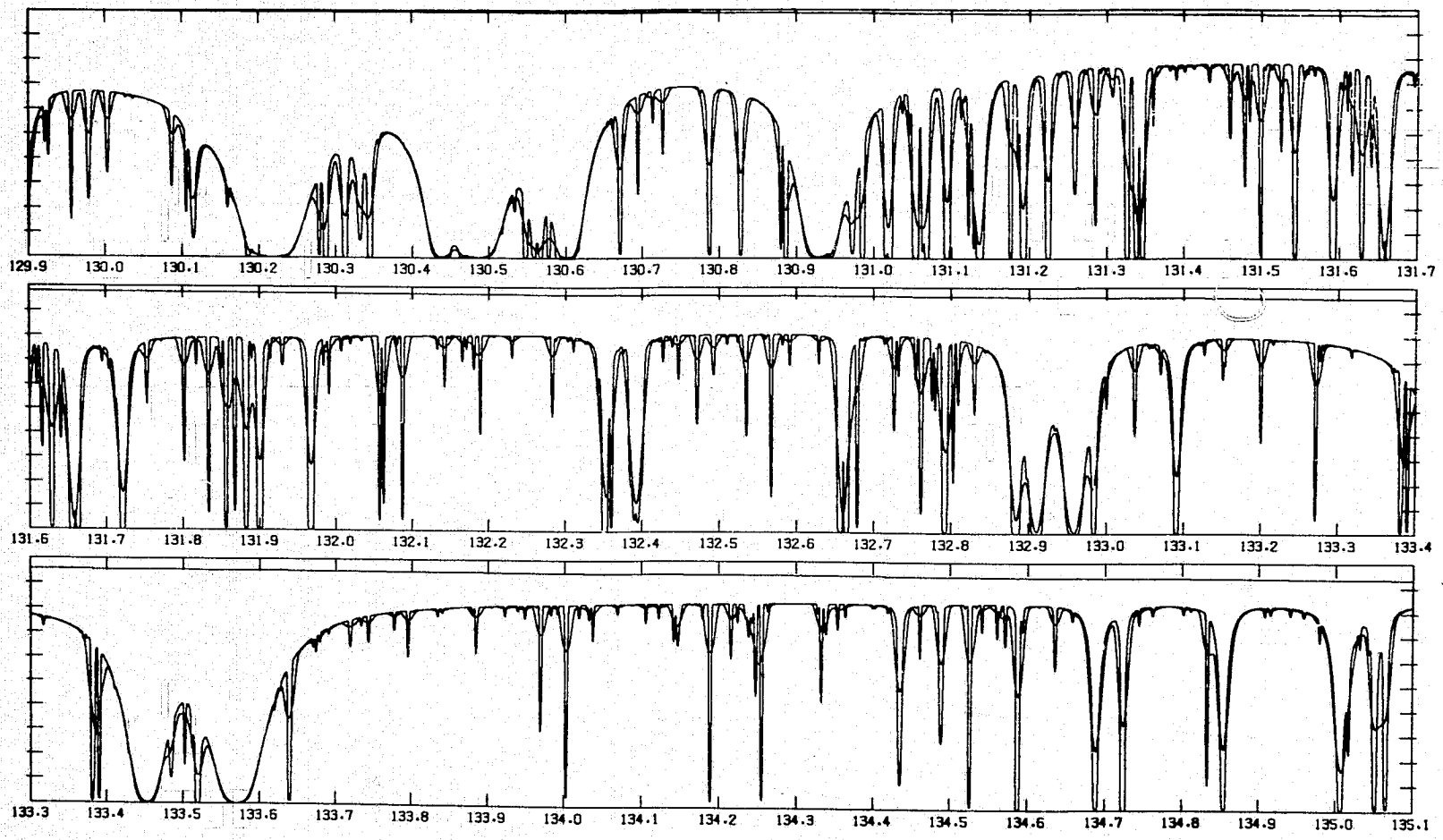

Figure 4. Calculated spectrum for Vega at 0 km/s and rotationally broadened to 25 km/s. The continuum is also shown. Full scale is 8.842E7 ergs/cm^2/s/ster/nm.

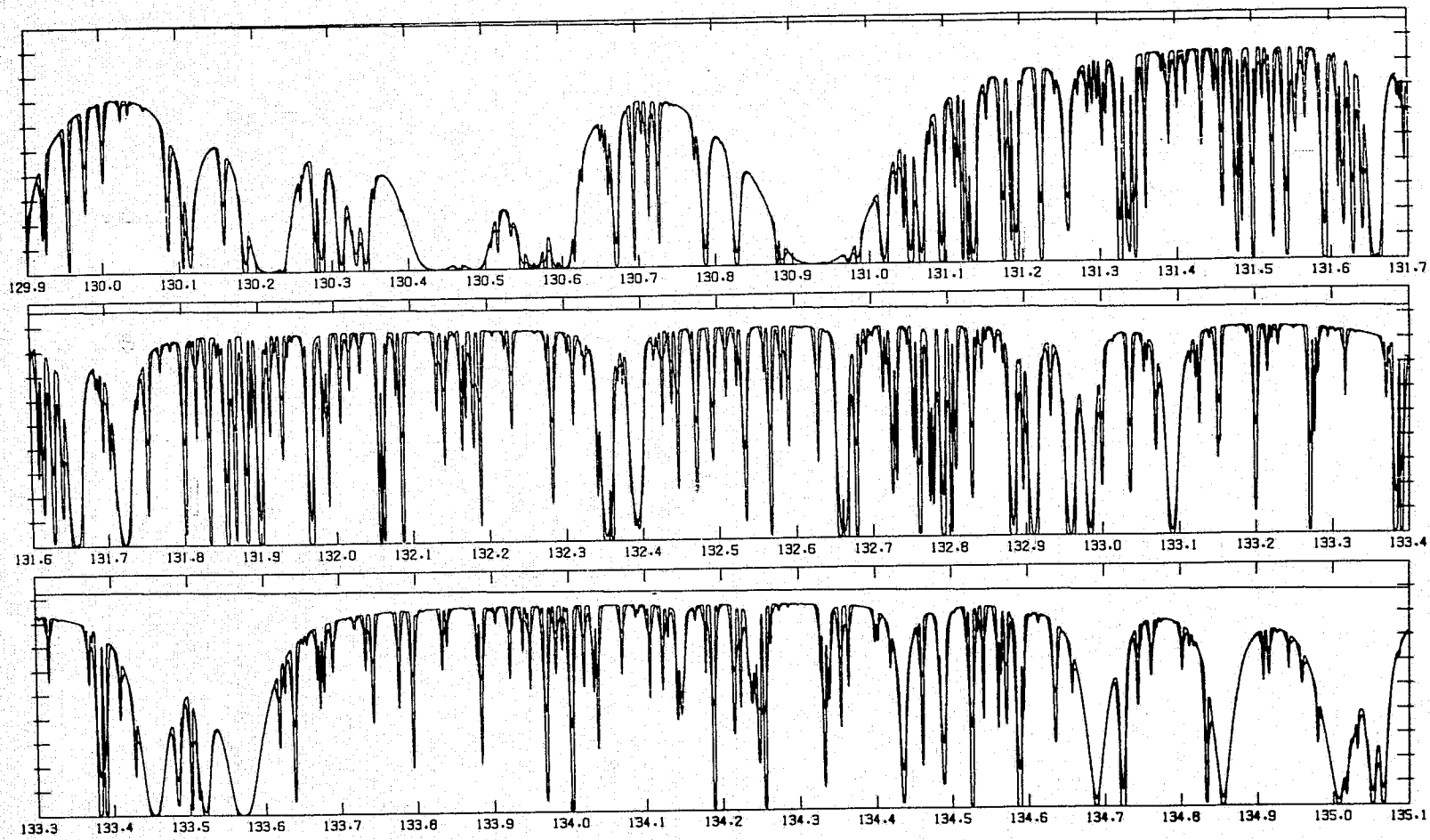

Figure 5. Calculated spectrum for Sirius at 0 km/s and rotationally broadened to 15 km/s. The continuum is also shown. Full scale is 1.320E8 ergs/cm^2/s/ster/nm.

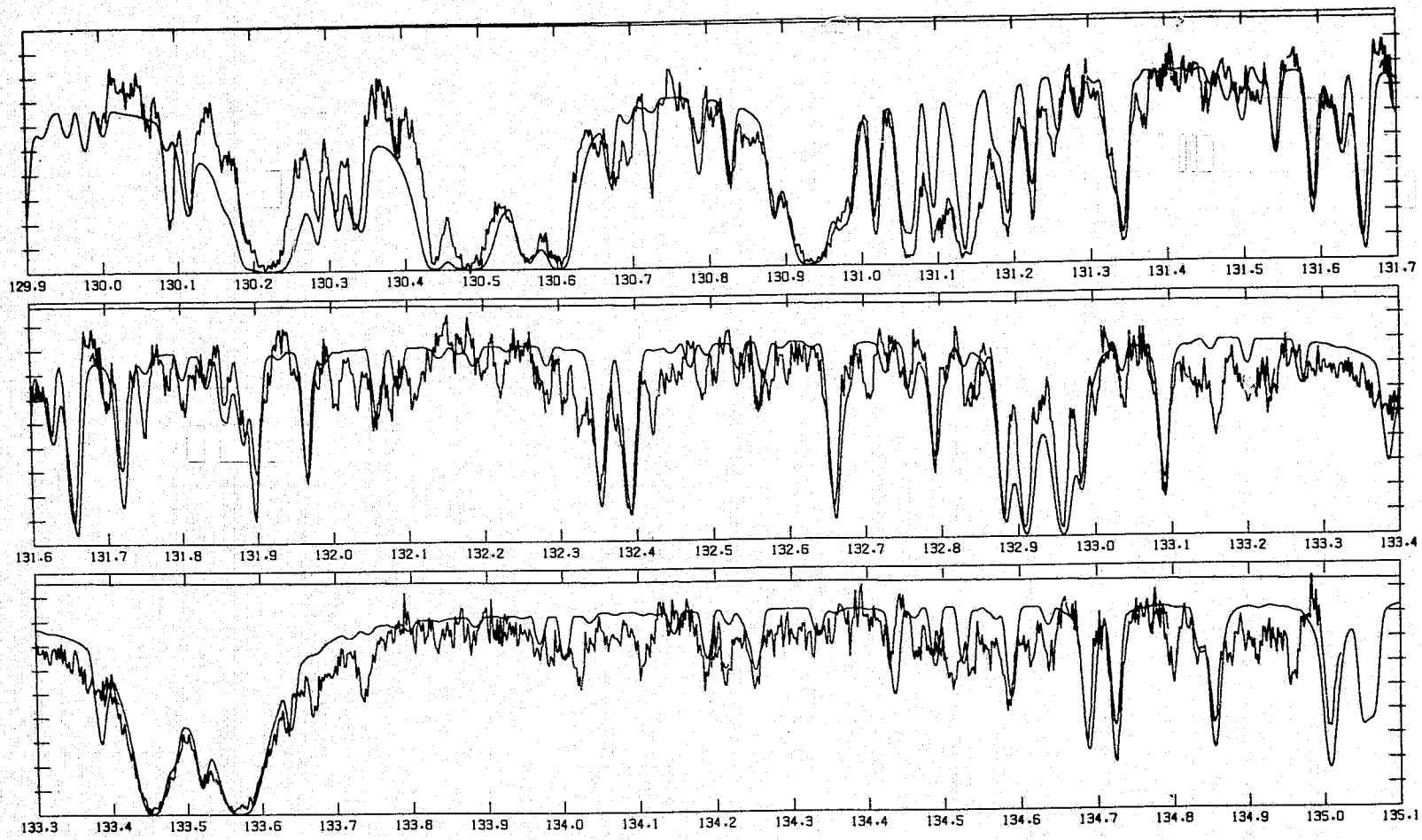

Figure 6. Calculated spectrum for Vega compared to the observations.

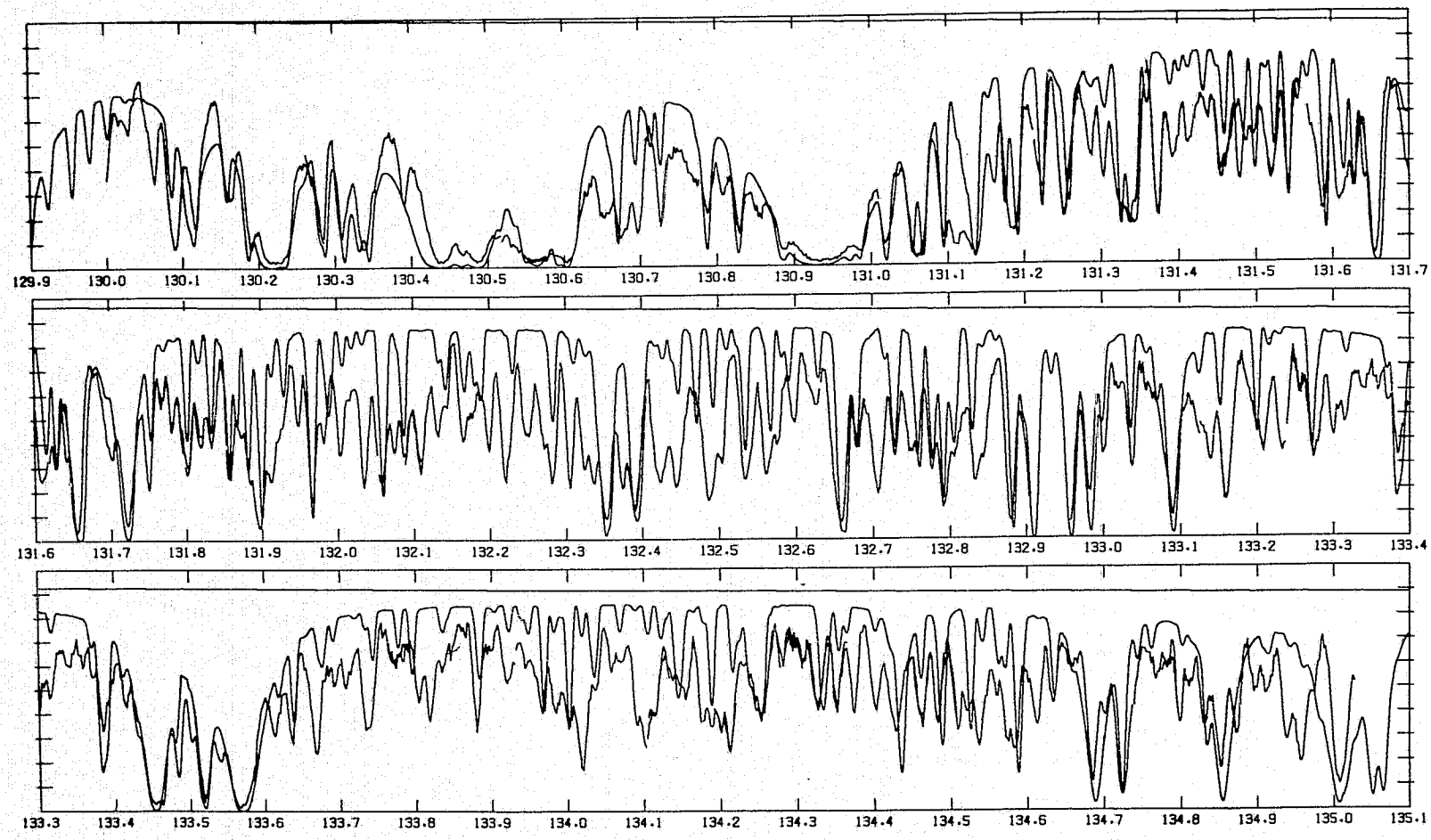

Figure 7. Calculated spectrum for Sirius compared to the observations.

Figure 8. Calculated spectrum for Vega compared to the observations with identifications. The labels consist of the last three digits of the wavelength, the symbol for the ion – atomic number plus charge, lower energy level in cm^{-1}, and the residual flux in per mil at line center in the unrotated spectrum.

Figure 8 (Continued)

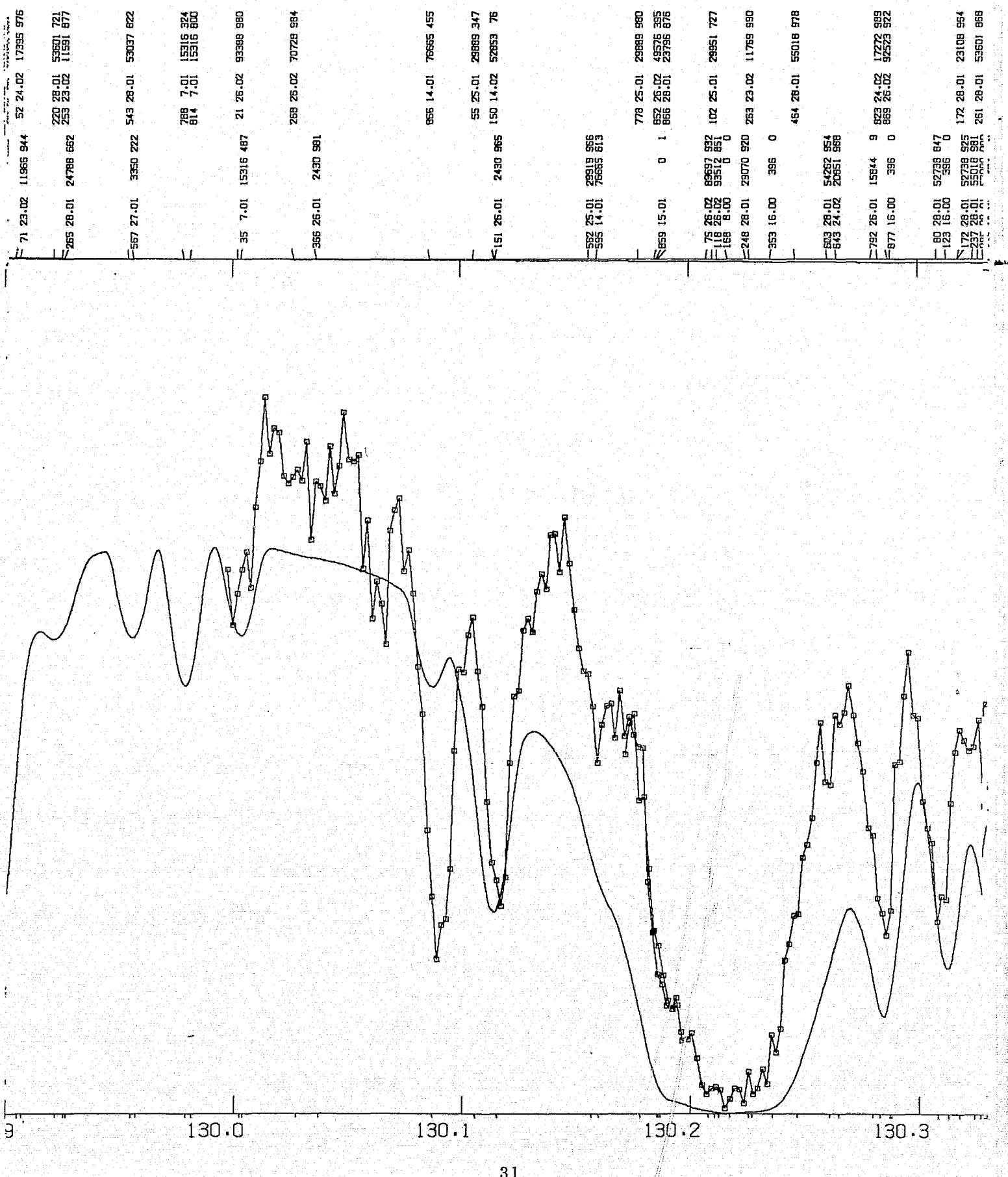

Figure 8 (Continued)

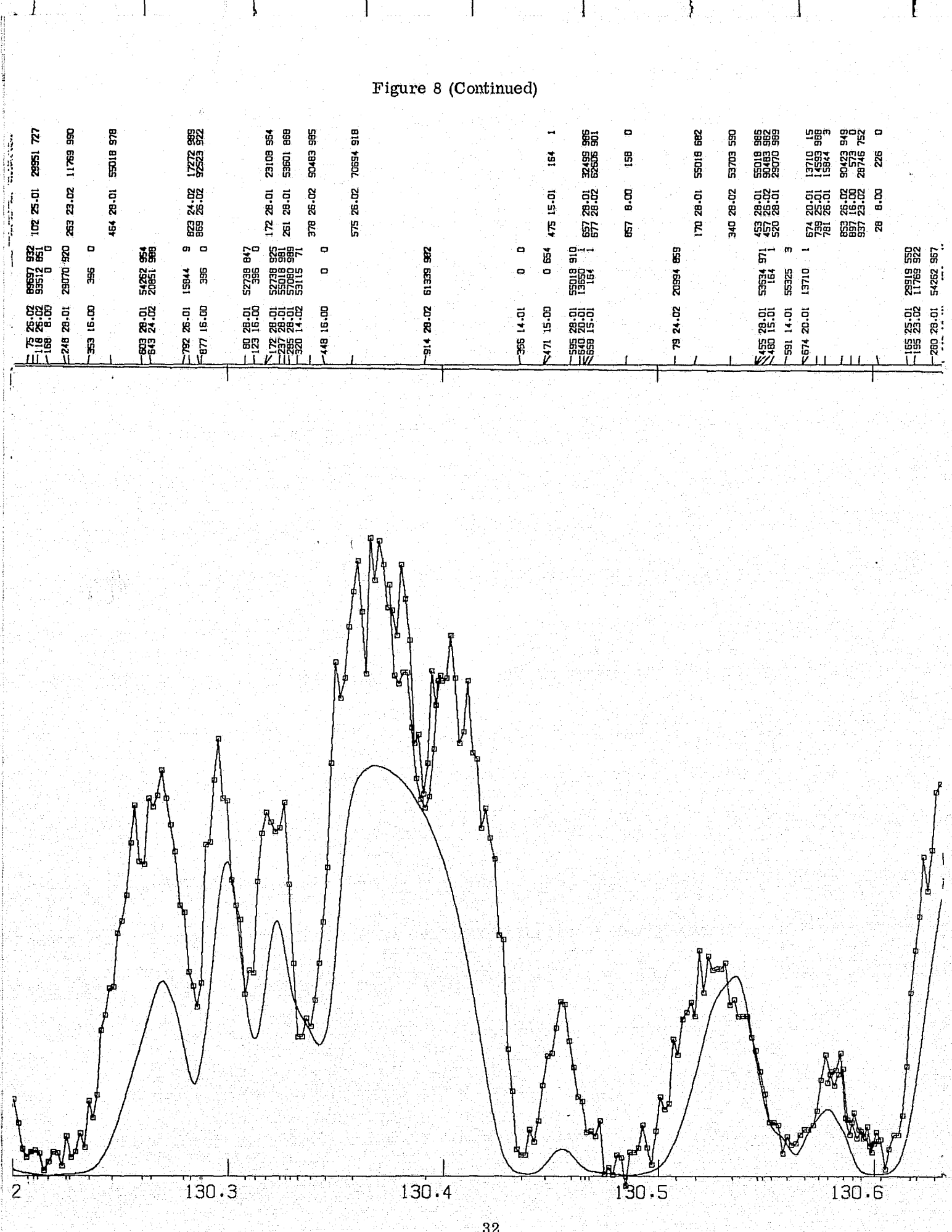

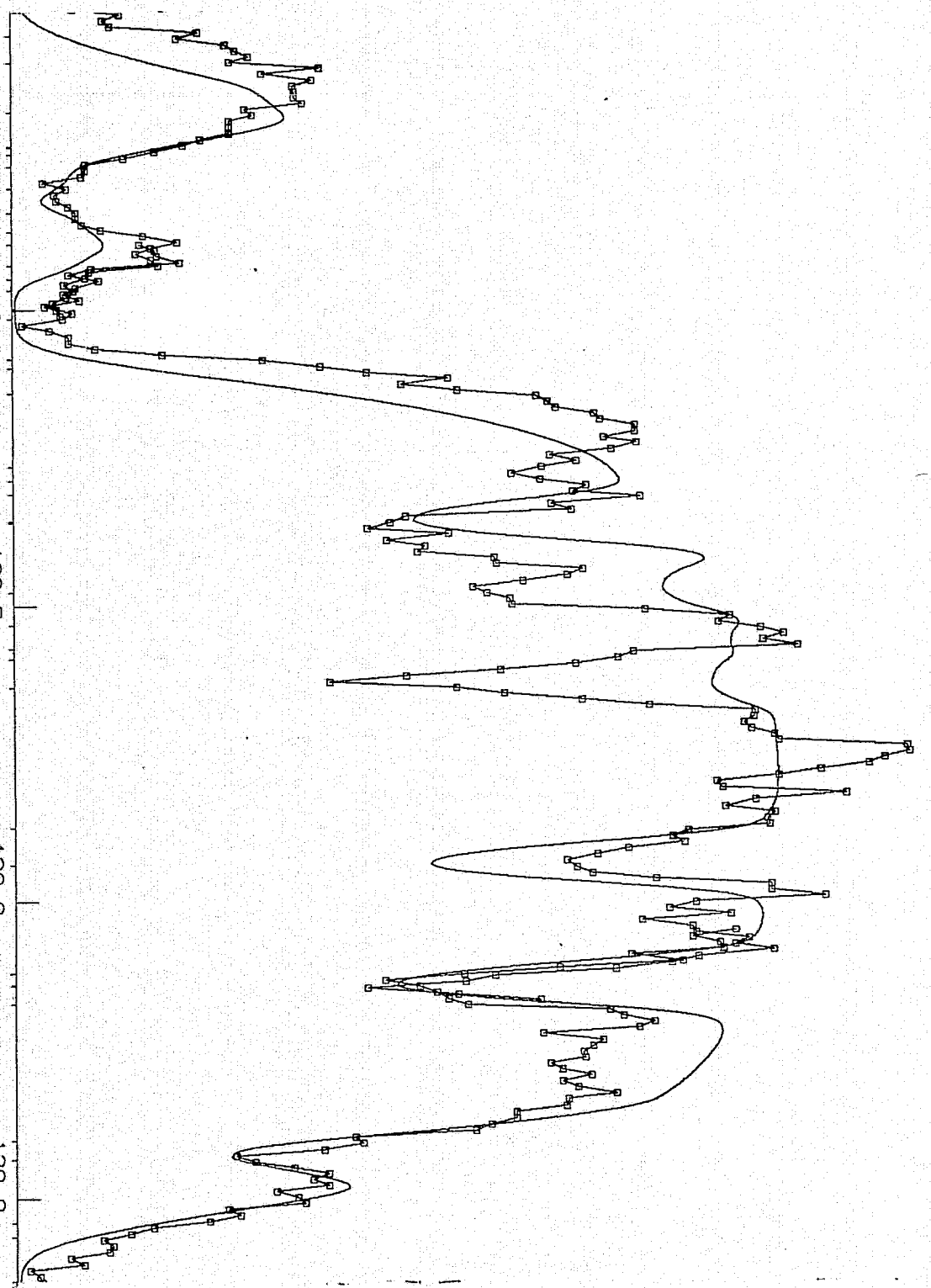

79 24.02 20994 859
170 28.01 55018 682
340 28.02 53703 590
455 28.01 53634 971
480 15.01 164 1
453 28.01 55018 986
457 26.02 90483 982
520 28.01 29070 989
591 14.01 55325 3
674 20.01 13710 1
674 20.01 13710 15
739 25.01 14593 988
781 26.01 15844 3
853 26.02 90423 949
897 16.00 573 0
937 23.02 28746 752
28 8.00 226 0
165 25.01 29919 550
195 23.02 11769 922
280 28.01 54262 967
529 28.01 54262 982
577 23.02 28746 976
621 28.01 52738 900
710 25.01 29951 725
714 12.01 35669 21
952 27.01 4028 391
63 24.02 20851 974
145 28.01 54262 811
180 28.01 53634 988
277 28.01 54262 614
748 26.02 70694 956
875 12.01 35669 13
239 26.02 69783 988
279 12.01 35760 279
281 12.01 35760 12
342 26.02 70728 946
801 26.01 2837 57
866 28.01 0 0
79 28.01 57420 985
126 28.01 53601 989

Figure 8 (Continued)

Figure 8 (Continued)

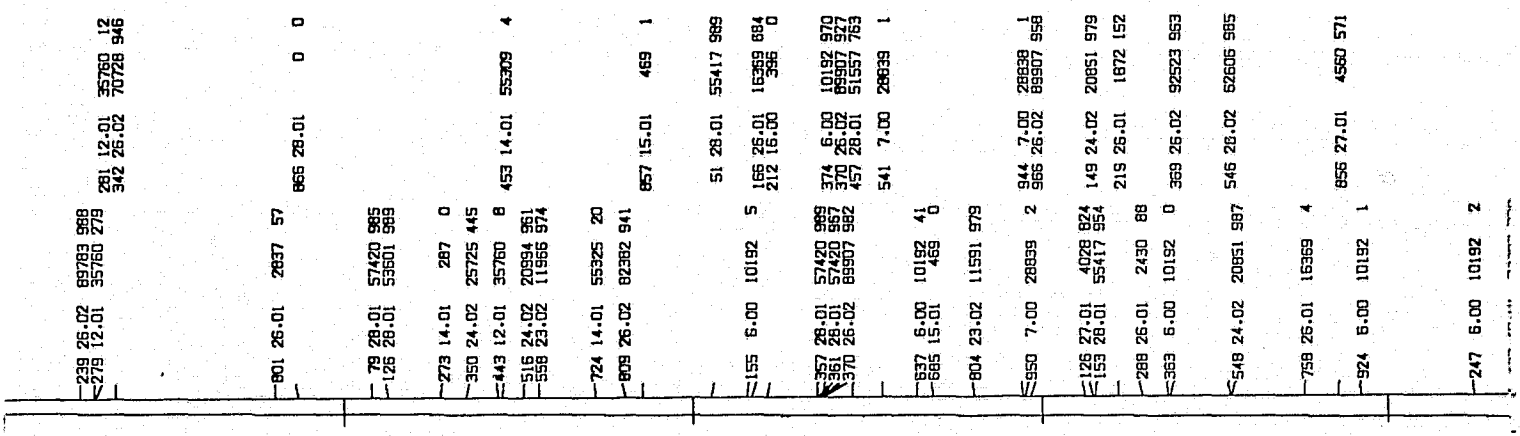

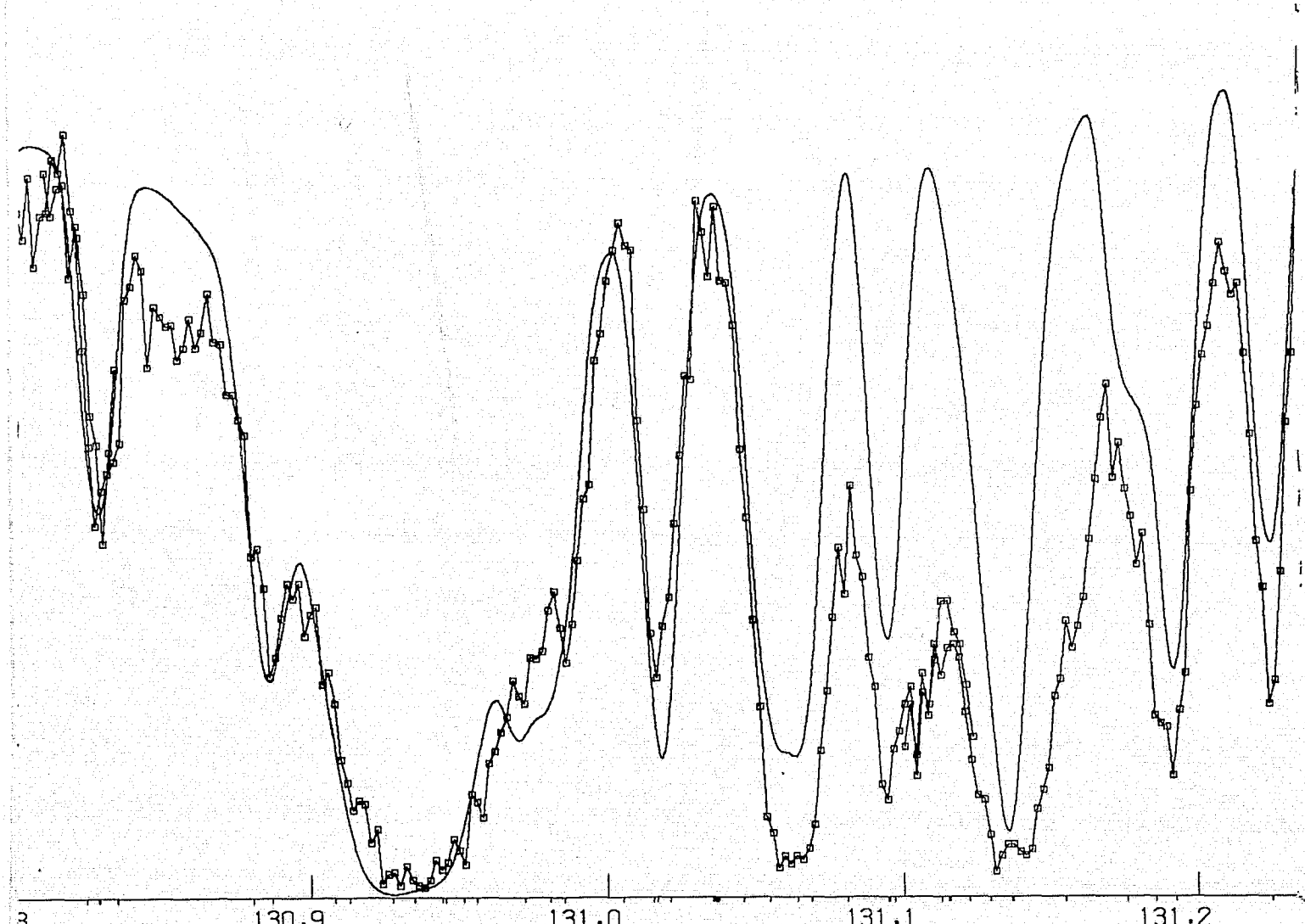

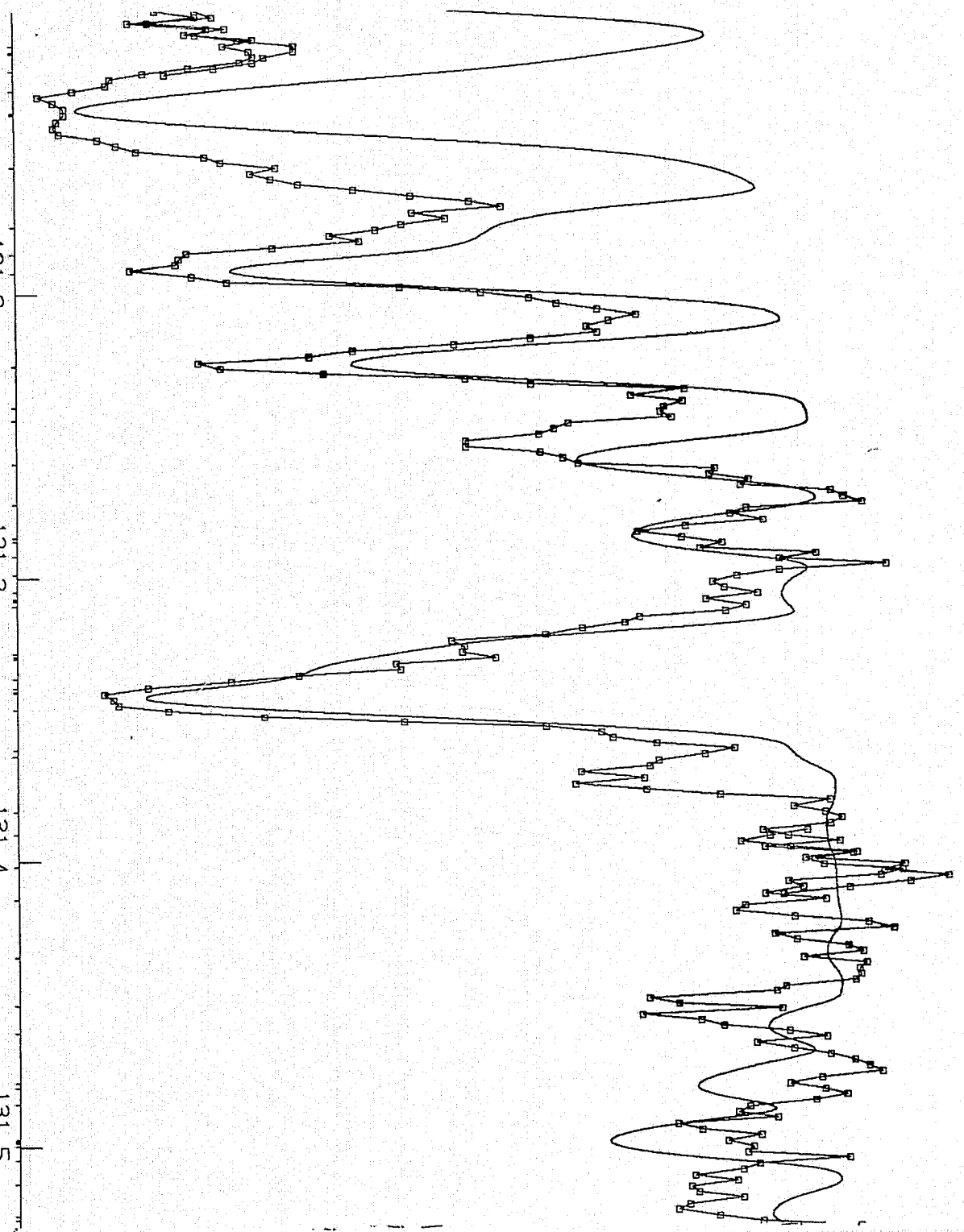

126 27.01 4028 824
153 28.01 55417 954
288 26.01 2430 88
363 6.00 10192 0
548 24.02 20851 997
758 26.01 16369 4
924 6.00 10192 1
247 6.00 10192 2
392 6.00 10192 970
440 28.01 54557 980
591 14.02 62884 323
866 7.00 28839 844
921 26.02 70725 973
46 26.02 63466 908
71 7.00 28838 912
96 26.02 89783 965
277 7.00 28838 912
354 23.02 12187 513
398 26.02 63466 979
607 26.01 3117 699
789 26.01 16369 379
848 28.01 53365 711
979 7.00 28839 912
995 15.00 0 17
129 26.02 63425 972
242 26.02 89907 997

149 24.02 20851 979
219 26.01 1872 152
369 26.02 92523 963
546 28.02 62606 985
856 27.01 4560 571
734 23.01 209 981
855 6.00 10192 194
986 26.02 70728 978
78 7.00 28839 912
267 16.00 573 1
283 7.00 26639 912
387 6.00 10192 3
403 28.01 53365 890
464 6.00 10192 2
629 6.00 10192 970
823 23.01 106 971
903 28.01 53365 926
17 24.02 20994 965
131 26.02 49576 978
332 26.02 63425 909
504 26.02 90423 979
601 26.02 40999 610
771 28.01 53365 733
974 7.00 28838 912
983 23.01 339 925
45 26.02 63466 970
242 26.02 89907 979

Figure 8 (Continued)

Figure 8 (Continued)

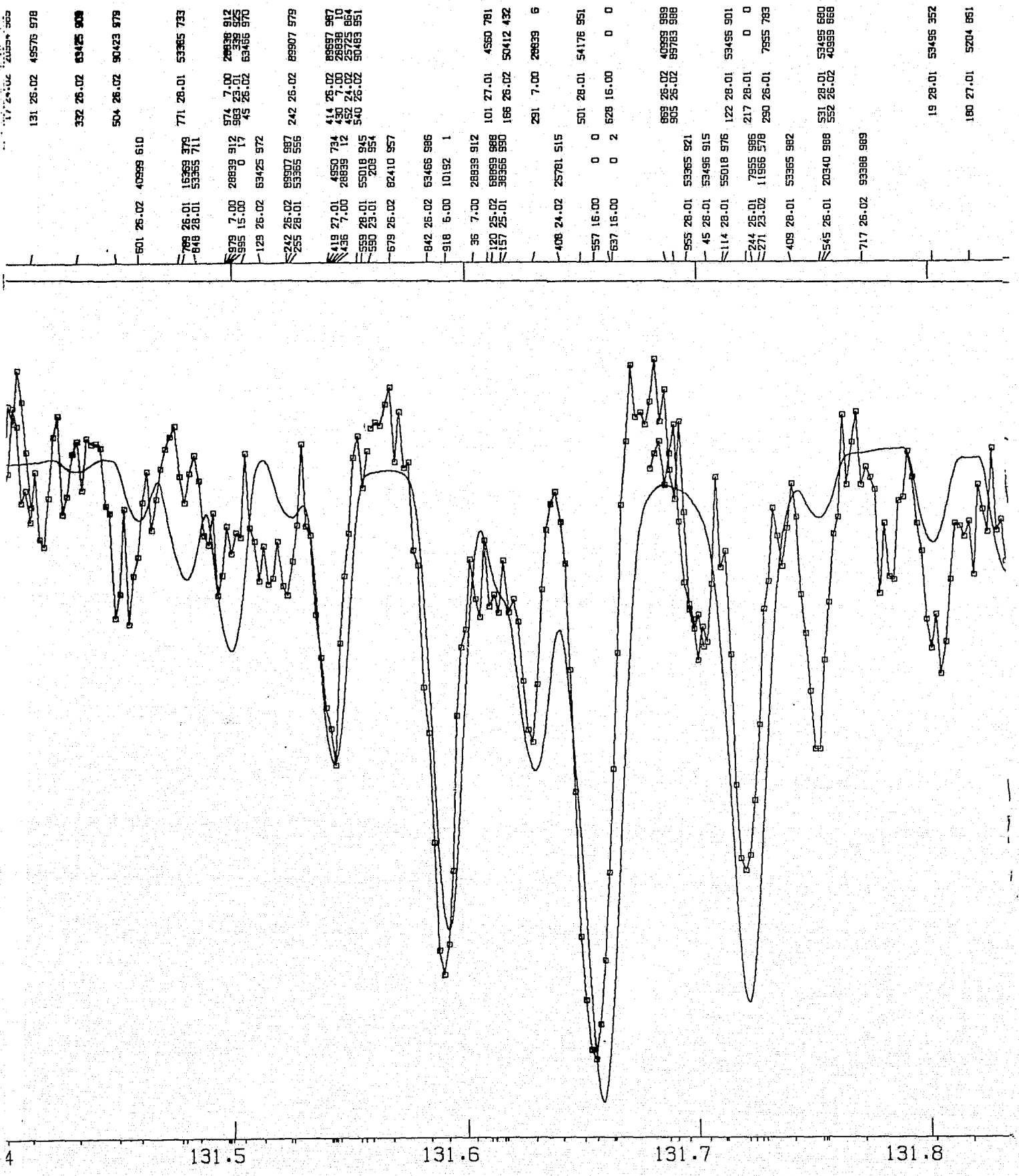

Figure 8 (Continued)

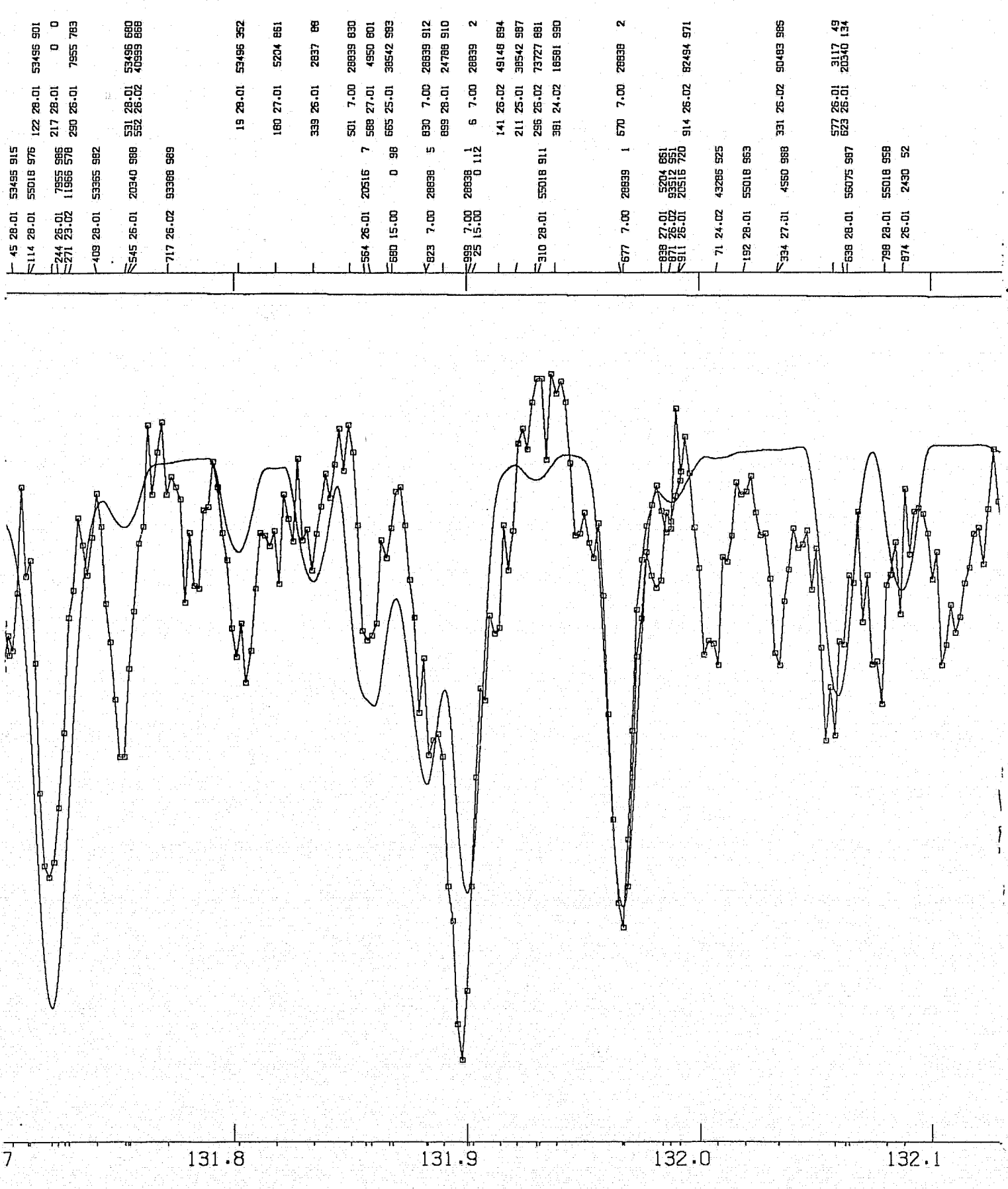

Figure 8 (Continued)

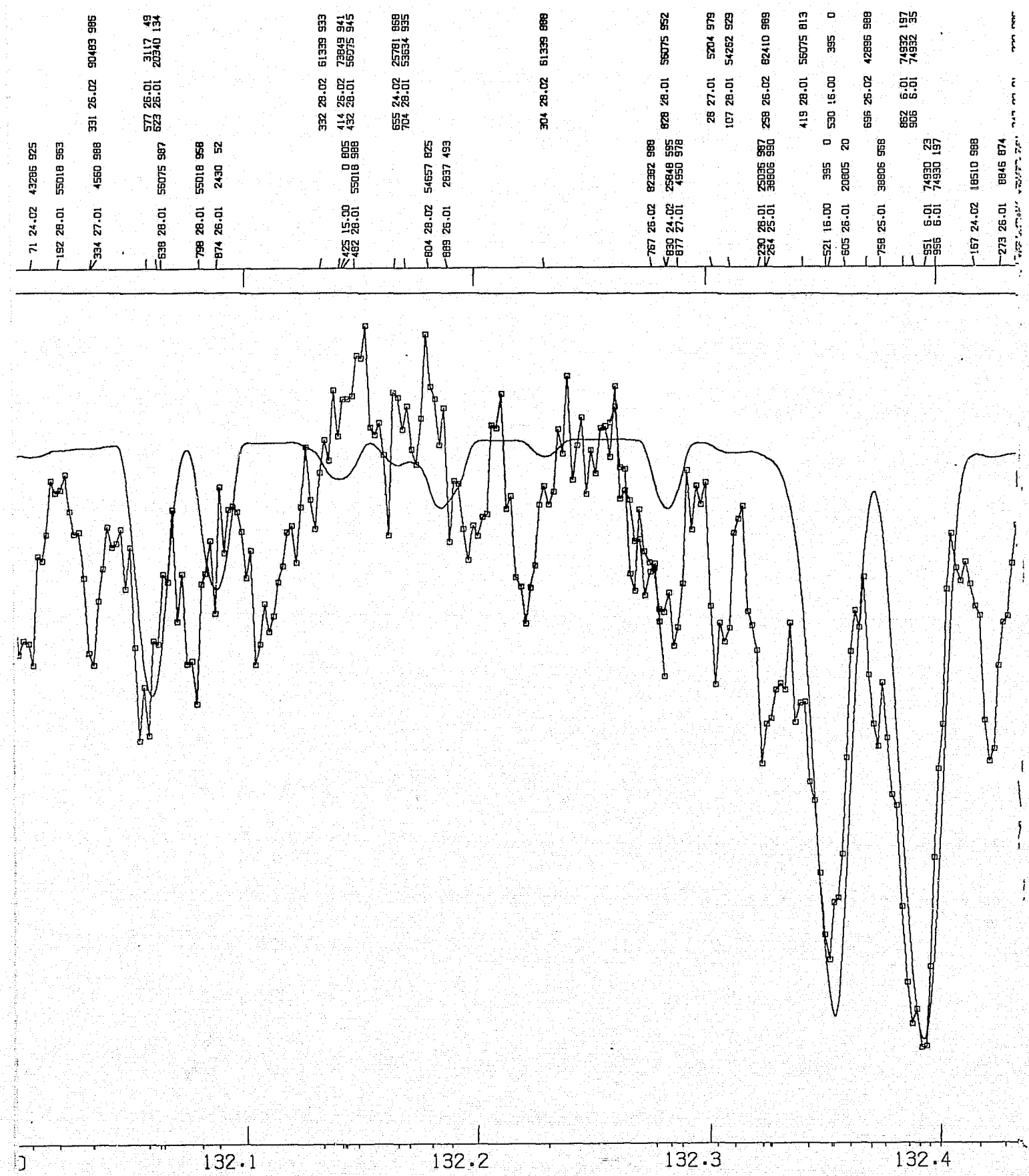

Figure 8 (Continued)

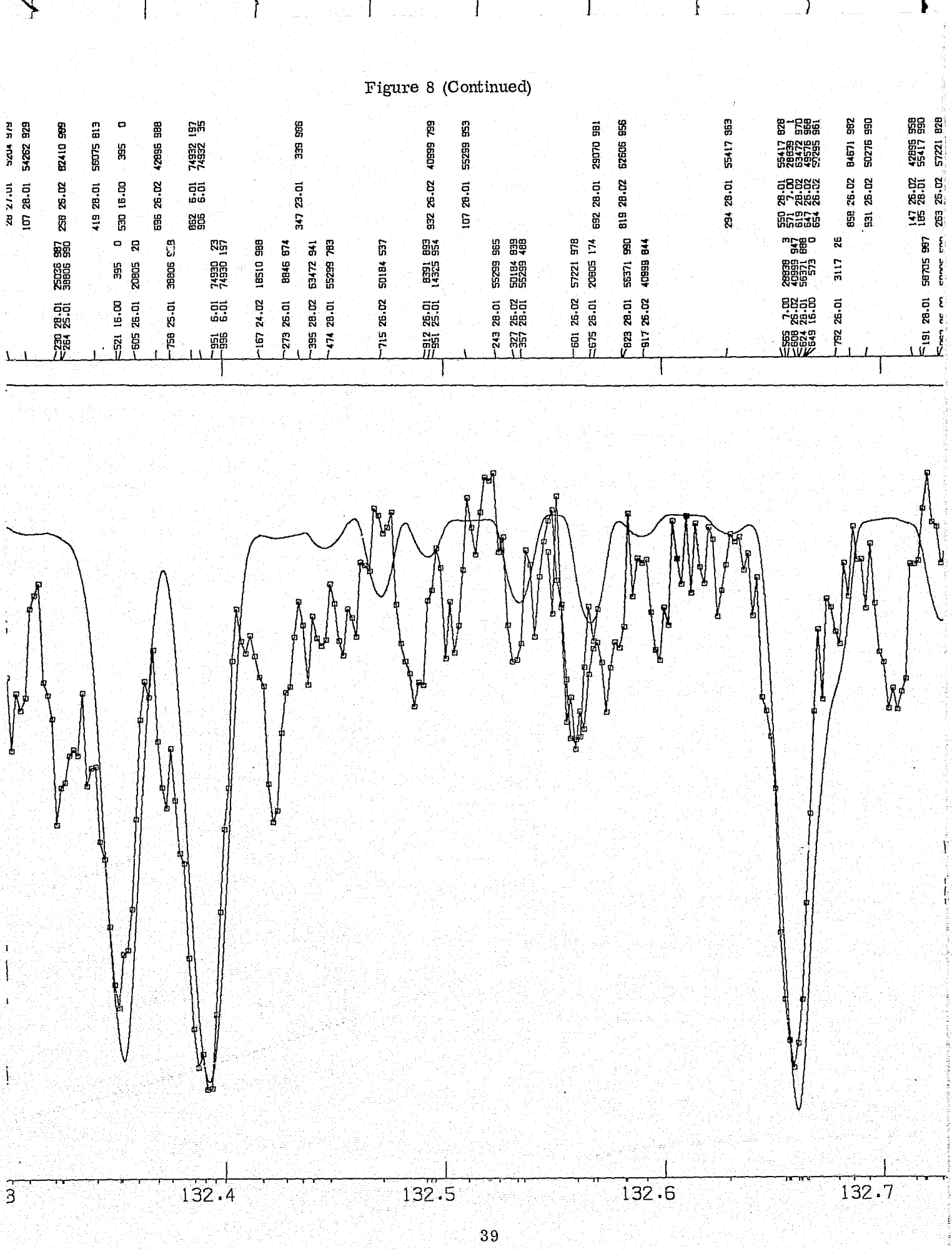

Figure 8 (Continued)

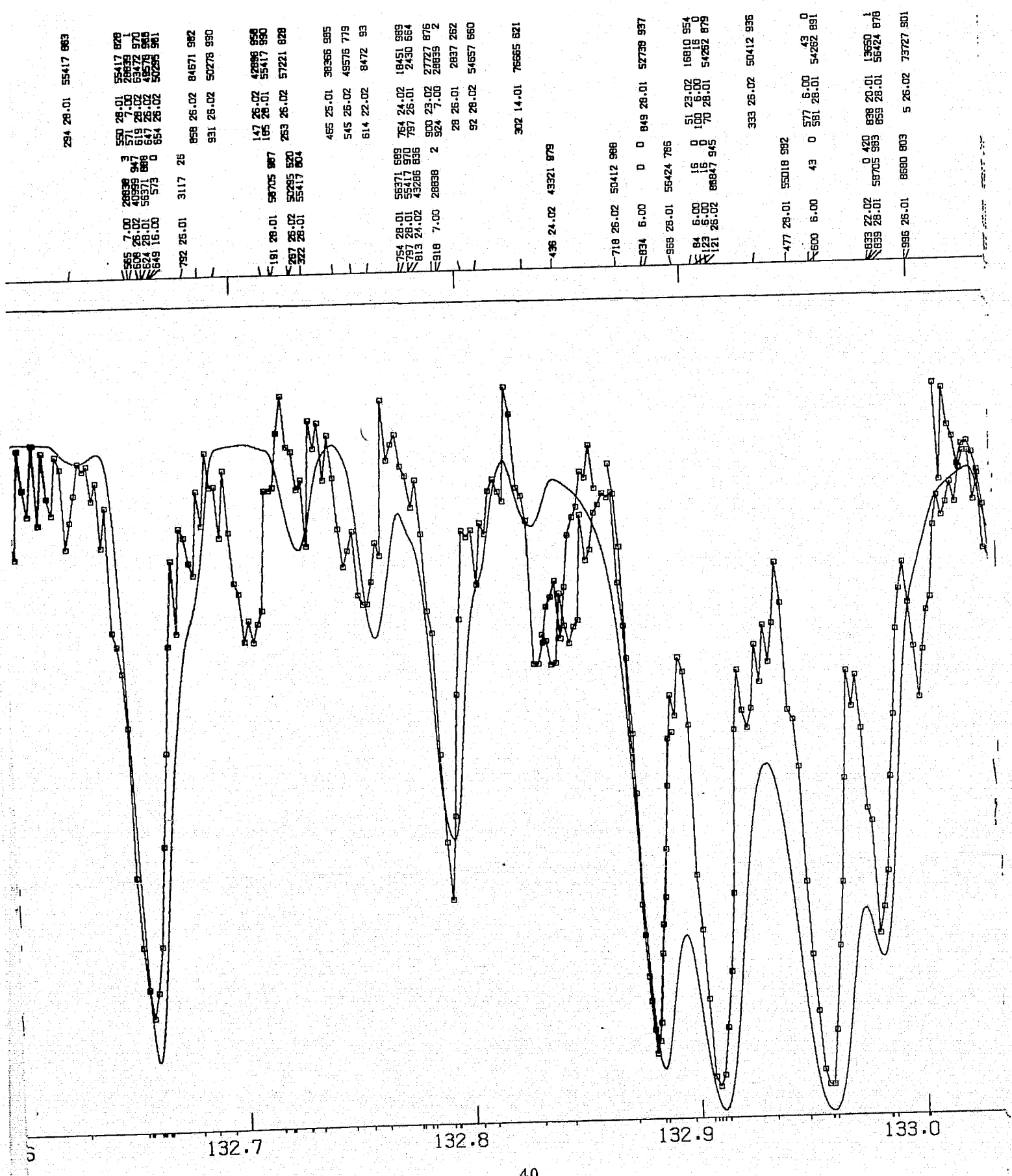

Figure 8 (Continued)

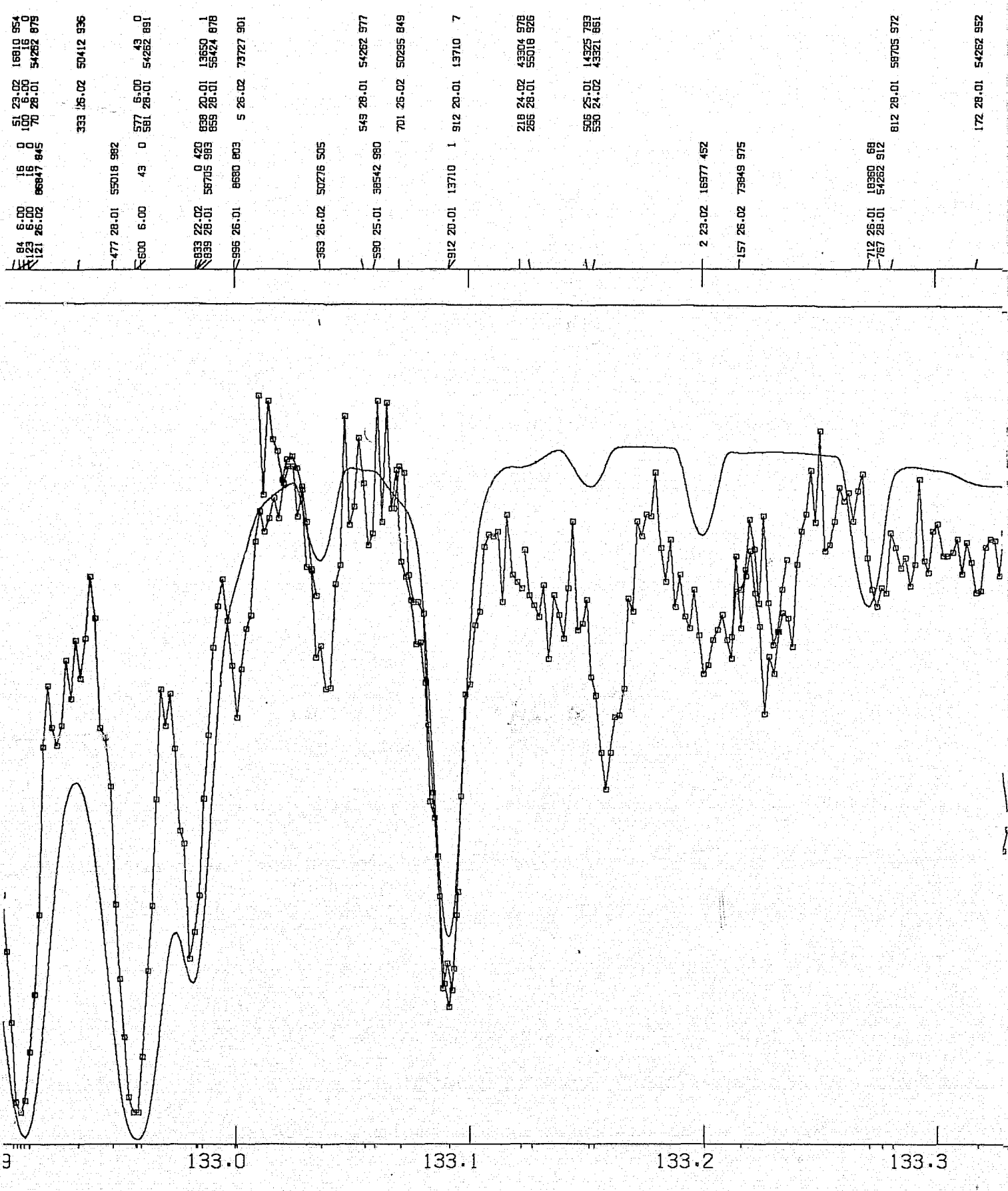

Figure 8 (Continued)

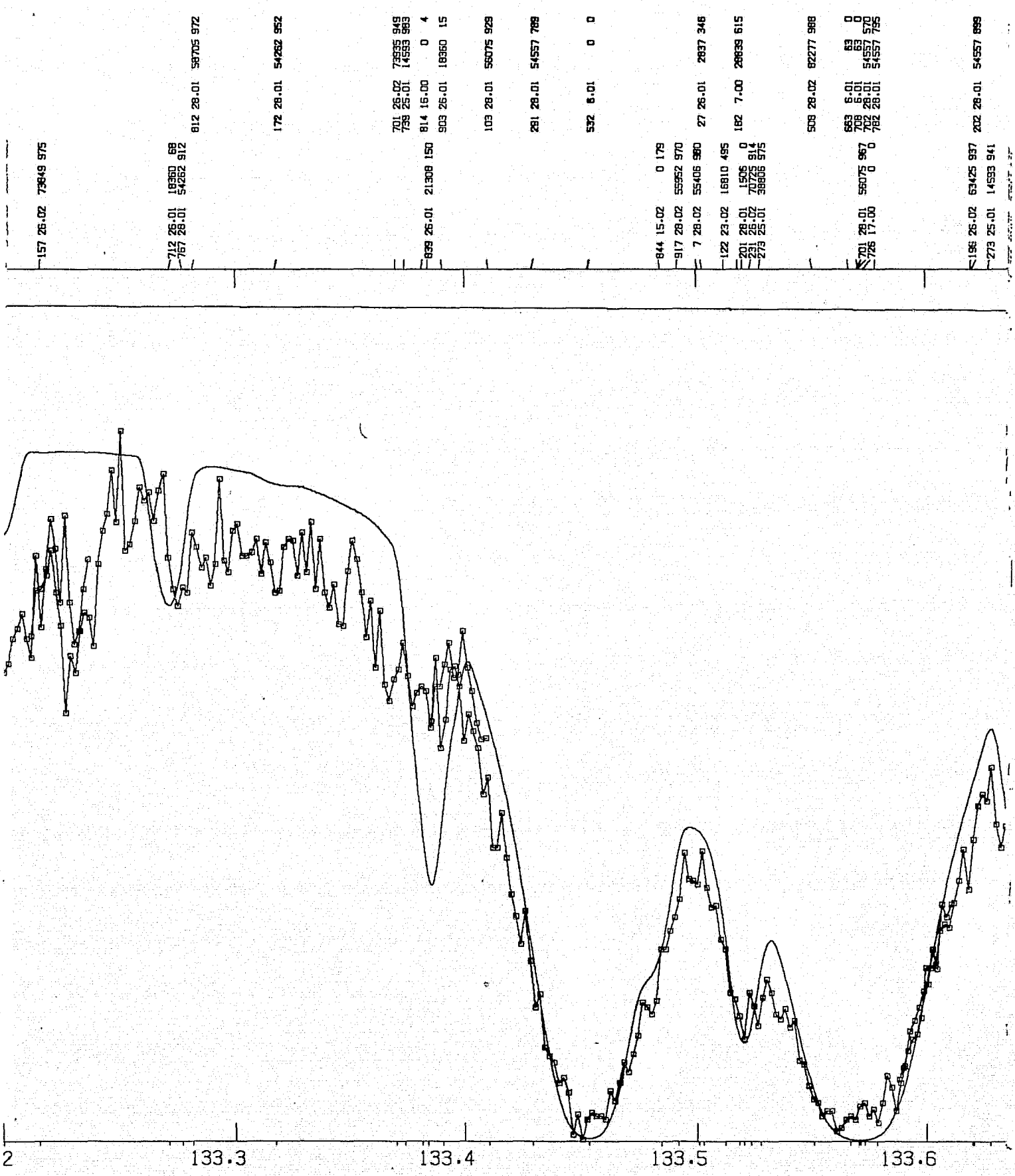

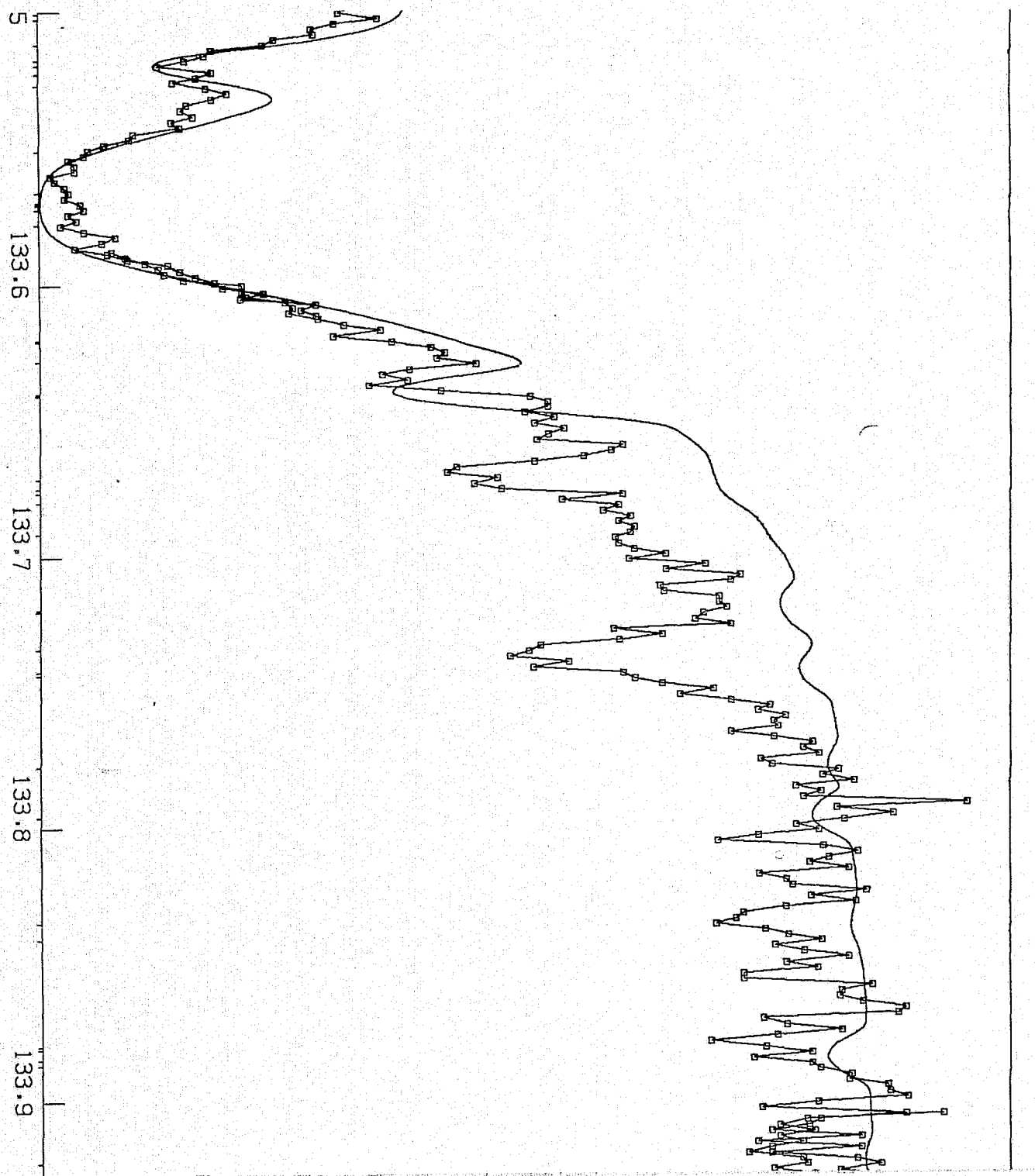

				27	26.01	2837	346
122	23.02	16810	495				
201	28.01	1506	0	182	7.00	28839	615
231	26.02	70725	914				
273	25.01	36806	975				
				508	28.02	82277	988
				663	8.01	63	0
				708	5.01	63	0
701	28.01	56075	967	702	28.01	54557	570
726	17.00	0	0	782	28.01	54557	795
196	26.02	63425	937	202	28.01	54557	899
273	25.01	14593	941				
394	7.00	28838	371	401	7.00	28839	14
				706	26.01	21251	939
760	28.01	25036	985	743	26.01	21430	899
793	26.02	73849	931				
911	28.02	82172	960				
191	7.00	28838	912	199	7.00	28839	912
				338	26.01	21581	957
435	26.02	50184	848	422	25.01	14325	987
				773	24.02	43304	900
956	28.01	54557	827	960	28.01	56075	895
				347	26.02	50184	959
407	28.01	57080	977				
797	26.02	63494	976	807	26.02	63494	986
843	28.01	23108	763	867	28.01	56075	947
				223	28.01	57080	952

Figure 8 (Continued)

Figure 8 (Continued)

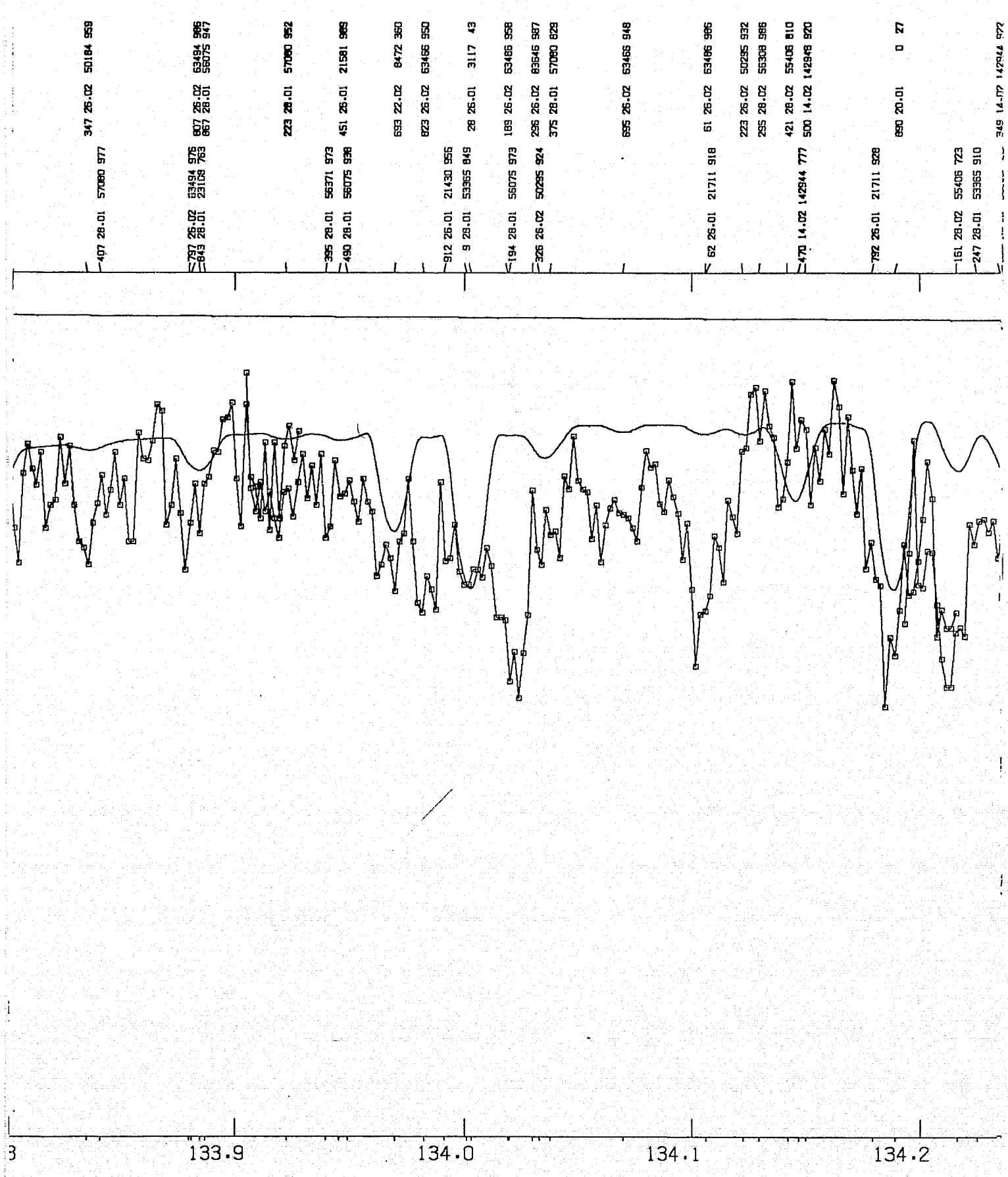

Figure 8 (Continued)

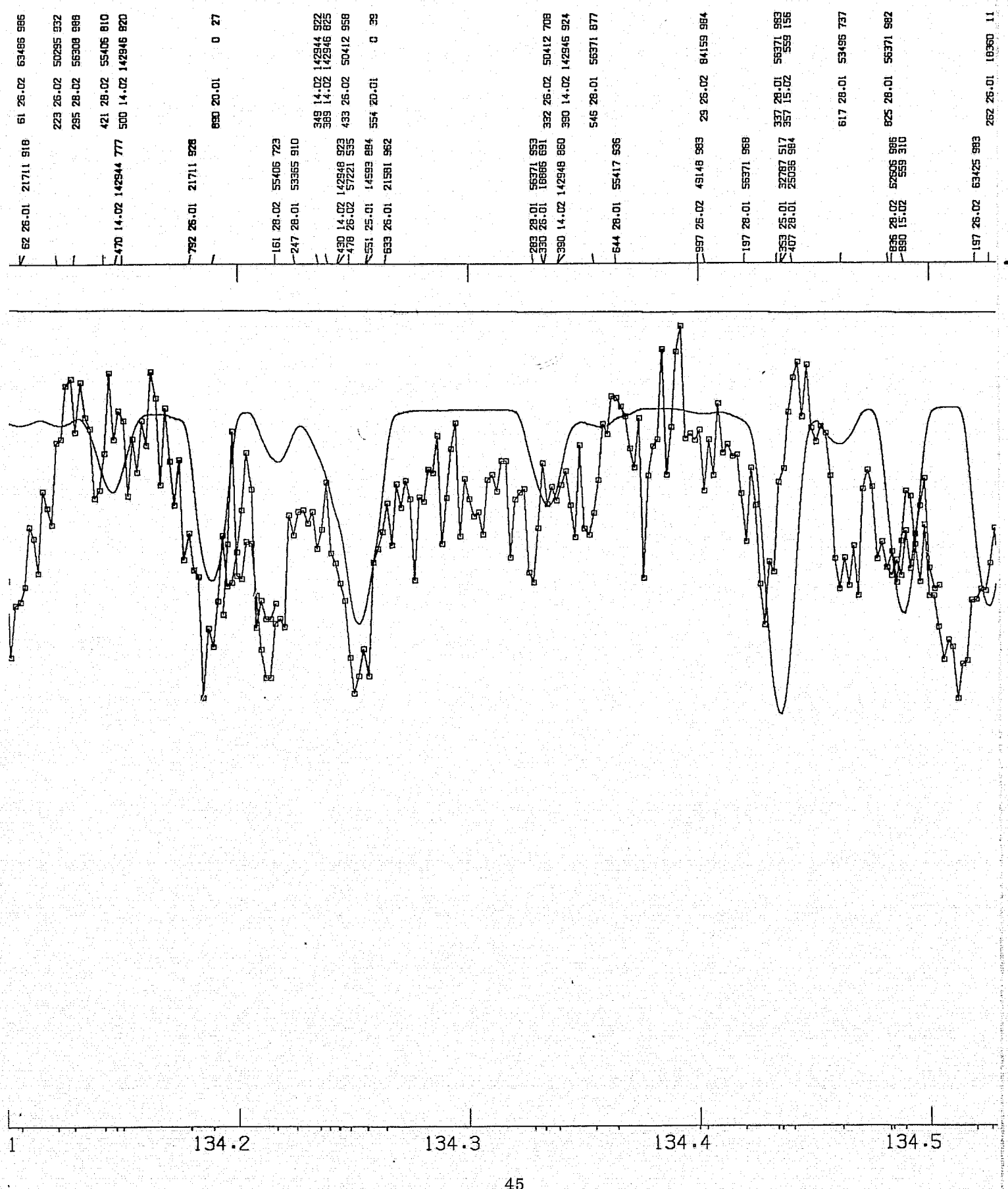

Figure 8 (Continued)

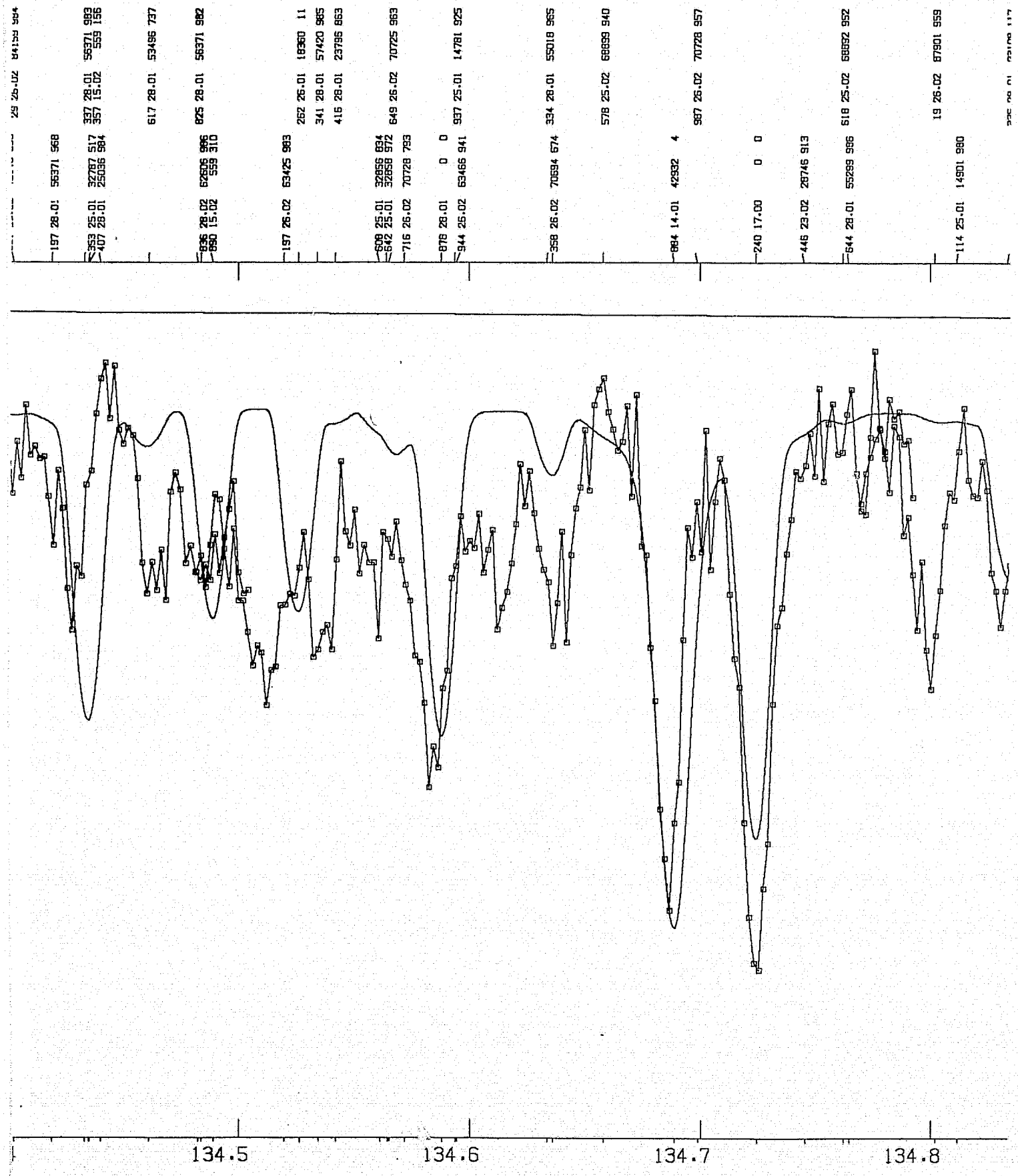

Figure 8 (Continued)

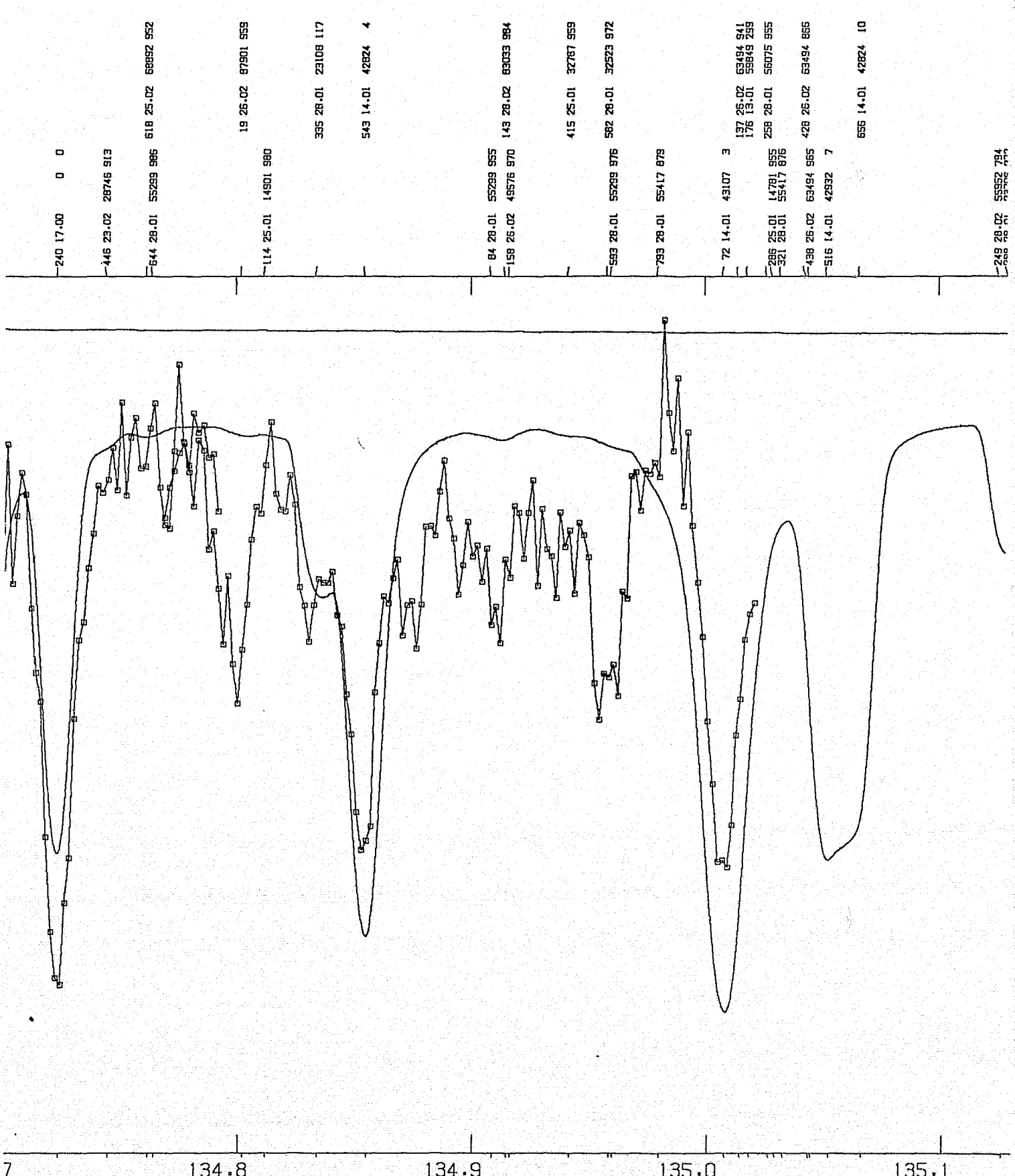

Figure 9. Calculated spectrum for Sirius compared to the observations with identifications. See Figure 8 for an explanation.

Figure 9 (Continued)

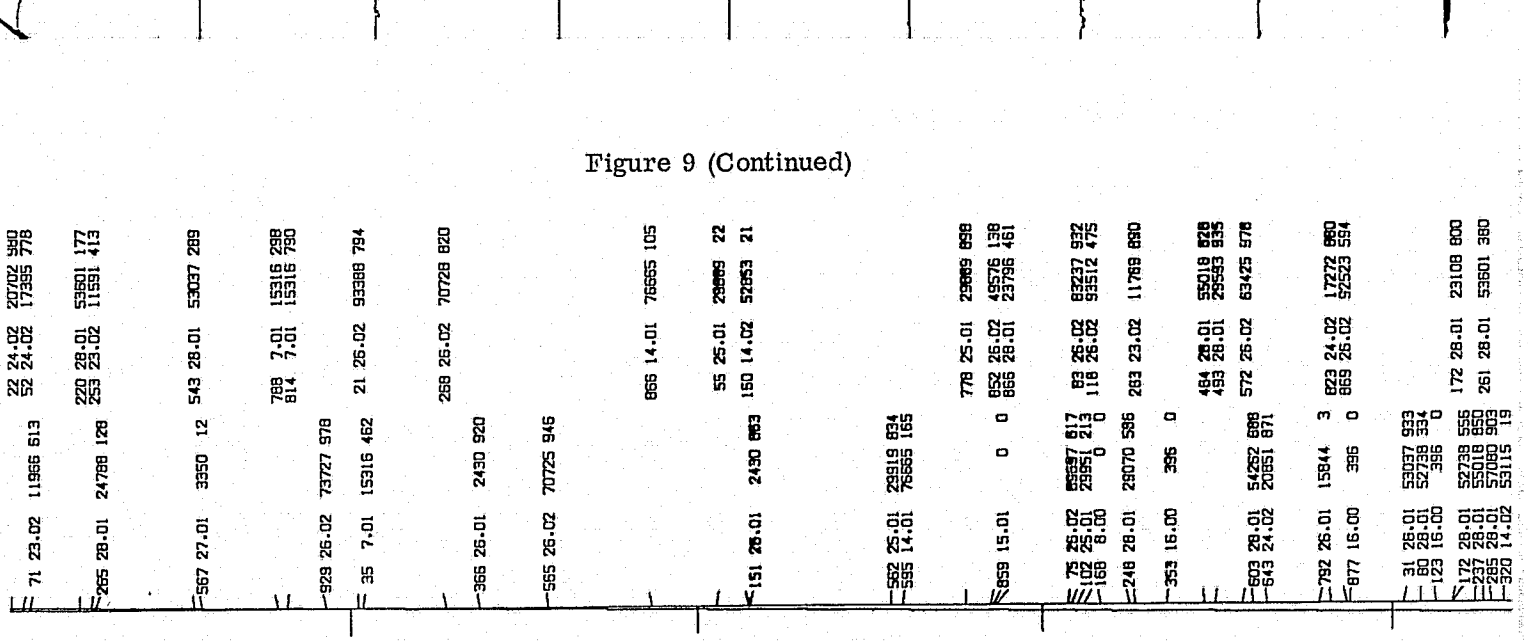

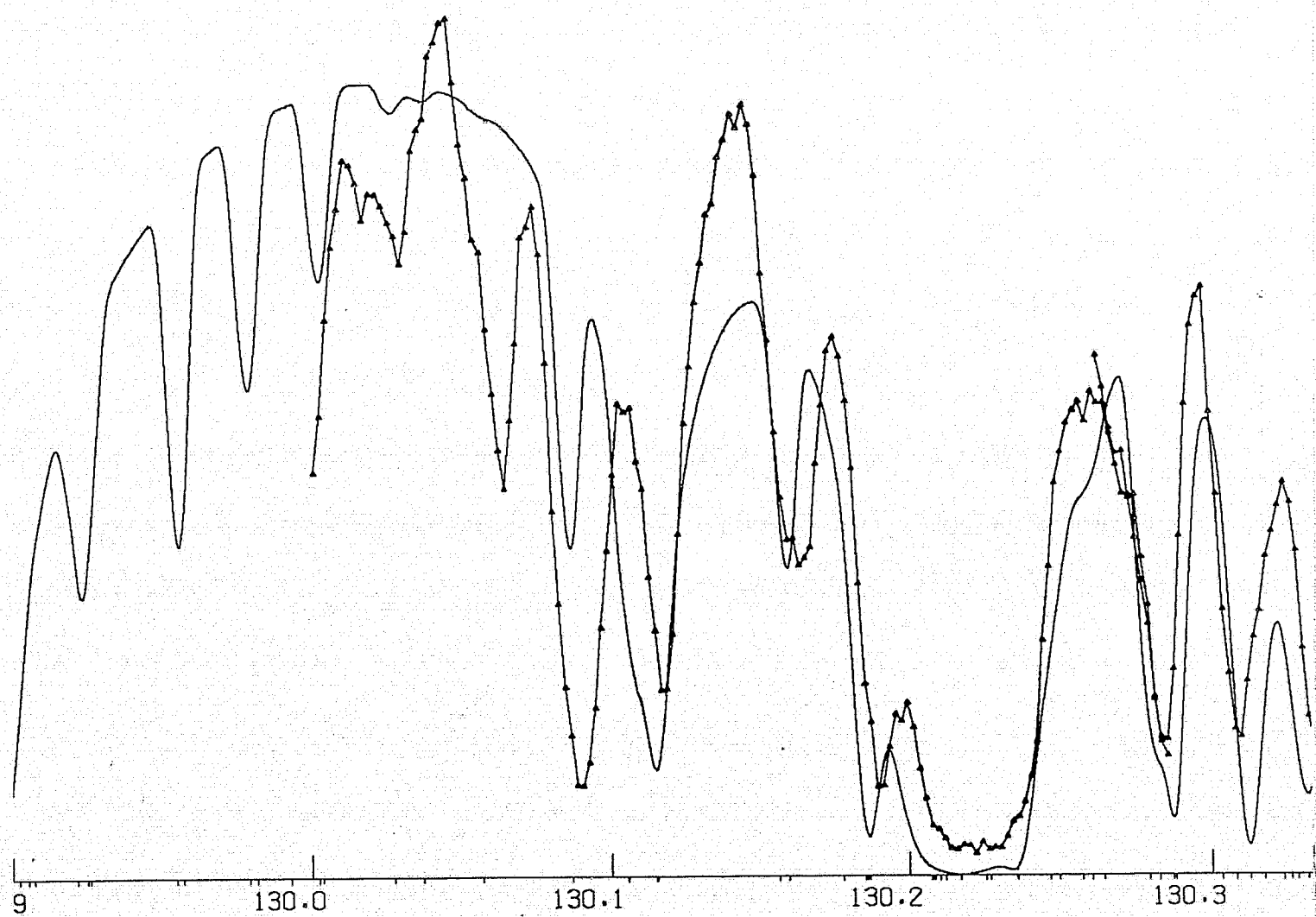

Figure 9 (Continued)

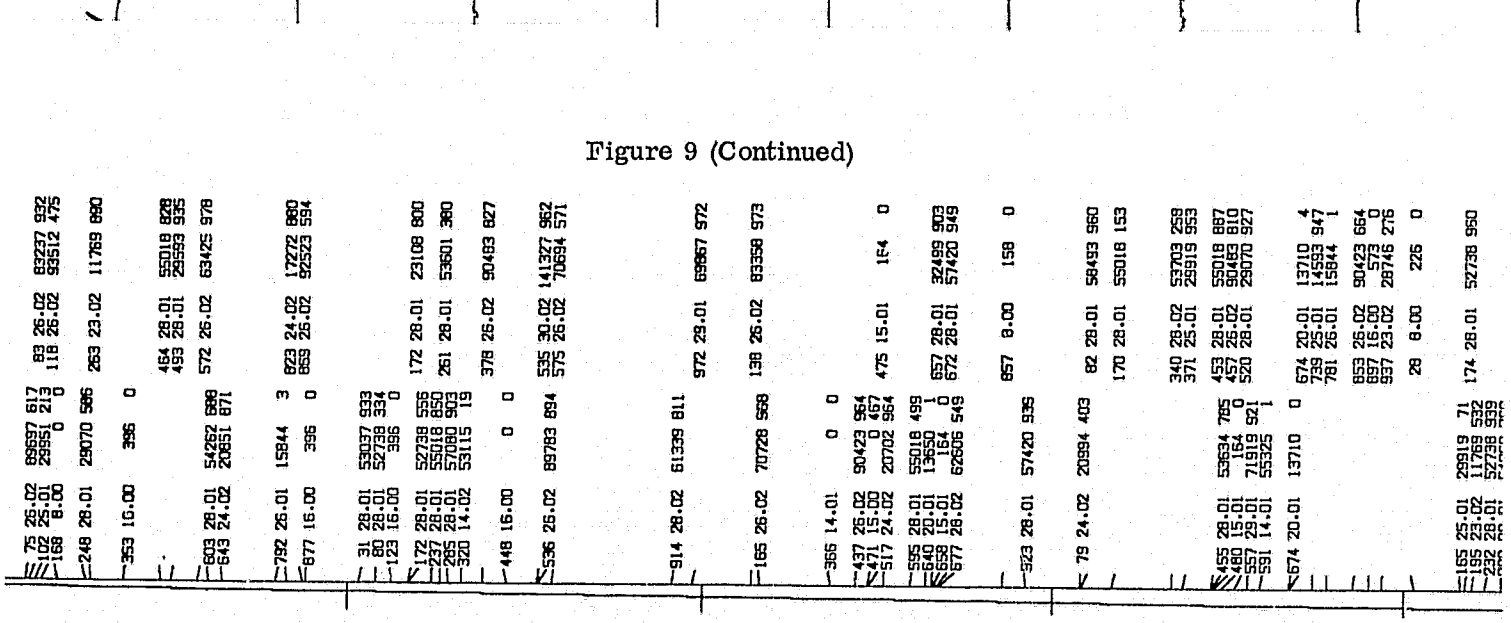

Figure 9 (Continued)

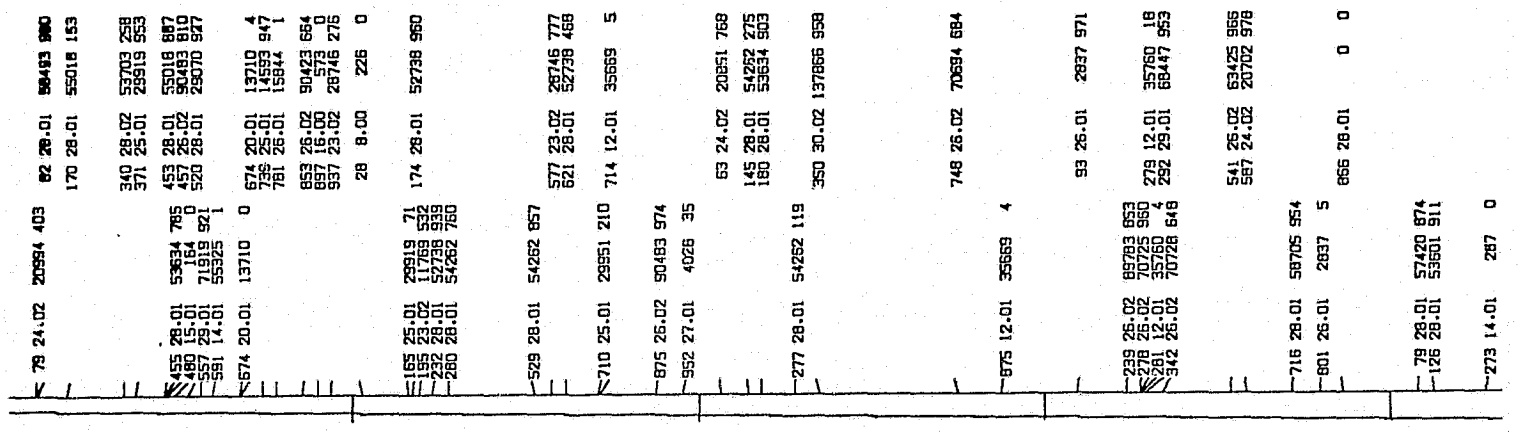

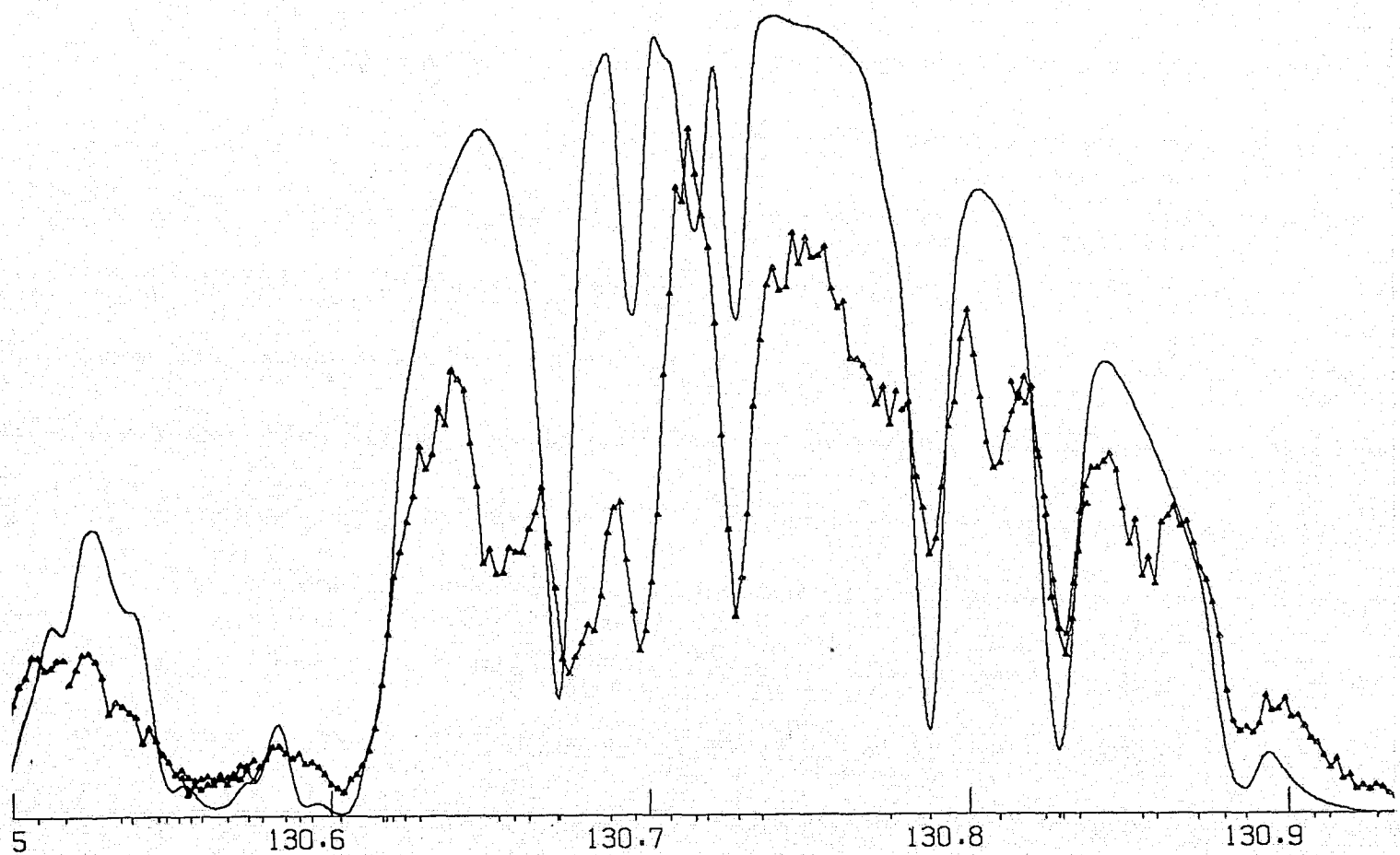

Figure 9 (Continued)

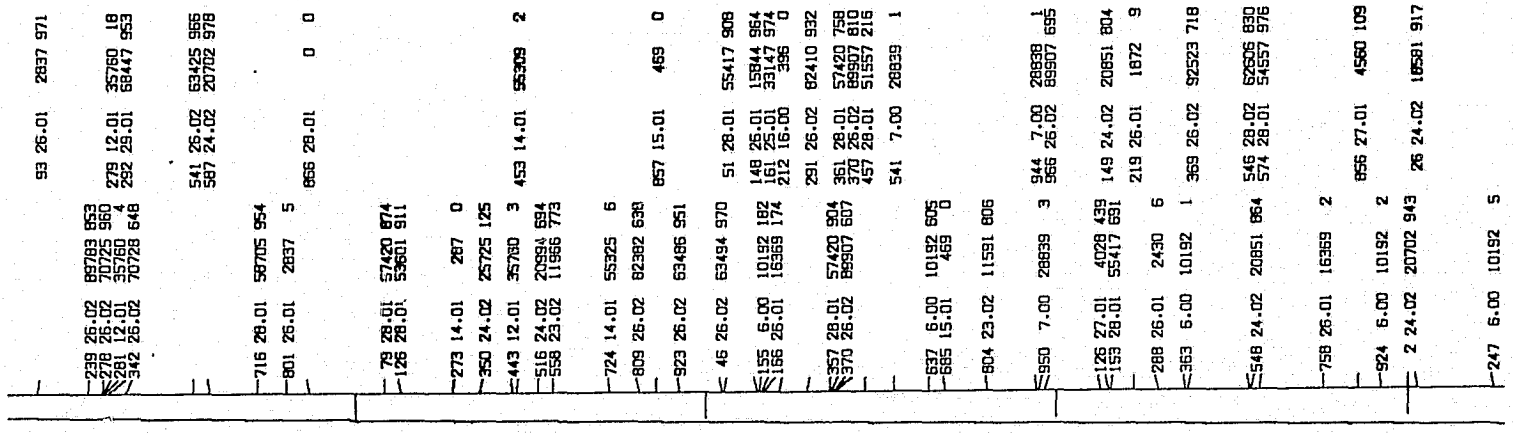

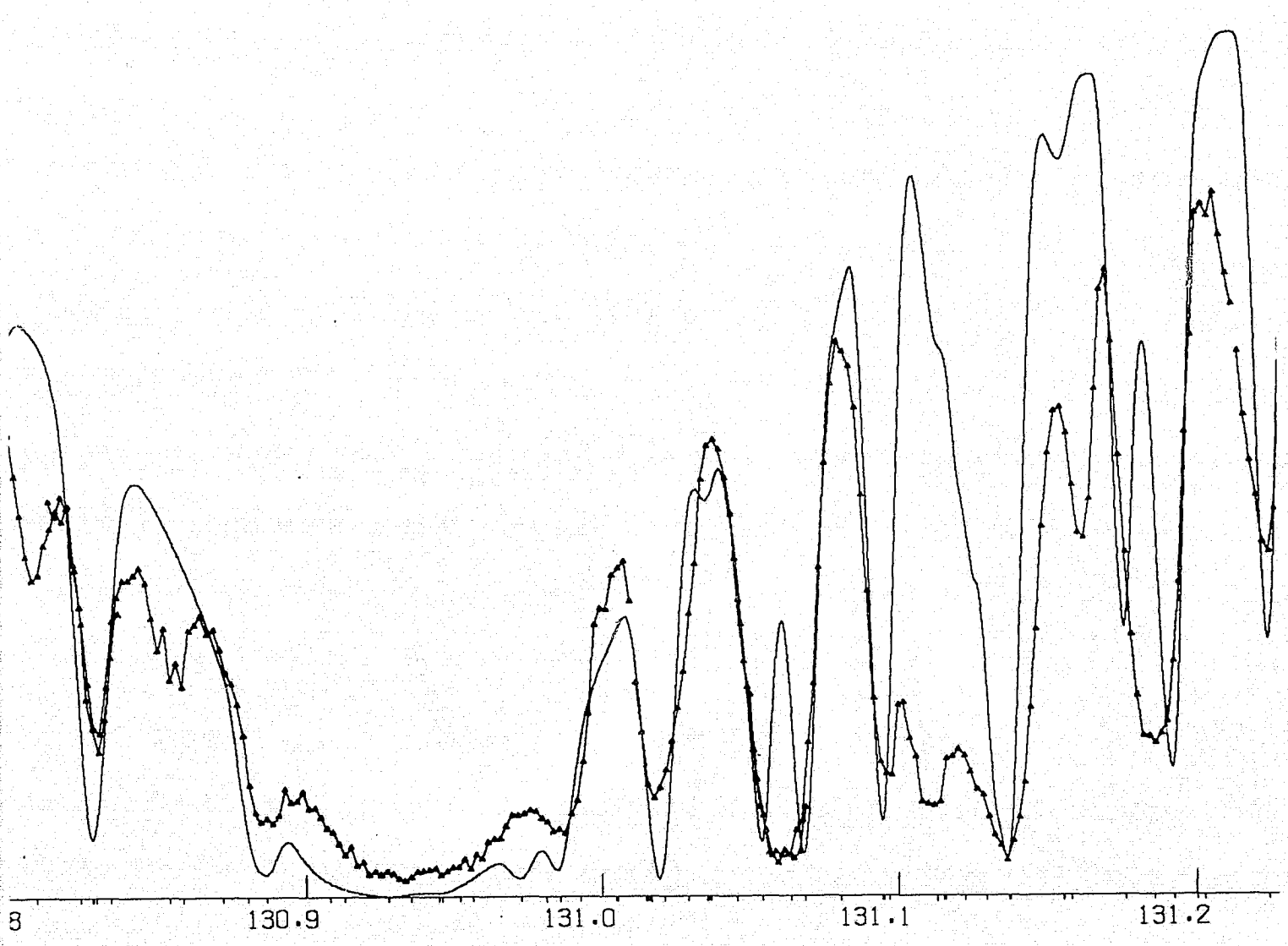

126	27.01	4028	439	149	24.02	20851	804
153	28.01	55417	691				
				219	26.01	1872	9
288	26.01	2430	6				
363	6.00	10192	1	369	26.02	92523	718
548	24.02	20851	864	545	28.02	62606	830
				574	28.01	54557	976
758	26.01	16369	2				
				856	27.01	4580	109
824	6.00	10192	2				
2	24.02	20702	543	26	24.02	16881	917
247	6.00	10192	5				
440	28.01	54557	921	445	26.02	63466	548
569	26.02	63494	898				
591	14.02	82884	131	606	23.01	36	975
663	26.02	82382	958				
735	28.01	58493	944	734	23.01	208	938
866	7.00	28839	935	855	6.00	10192	789
921	26.02	70725	760				
				986	26.02	70728	785
46	26.02	63466	548				
71	7.00	28838	965				
96	26.02	89783	726	78	7.00	28839	965
				217	28.01	58493	973
				267	15.00	573	0
277	7.00	28838	965	283	7.00	28839	965
354	23.02	12187	114				
398	26.02	63486	790	387	6.00	10192	45
				403	28.01	53365	439
				464	6.00	10192	11
607	26.01	3117	247				
				823	23.01	106	906
				868	23.02	11769	927
				909	28.01	53365	561
				17	24.02	20994	716
144	29.01	70841	979	131	26.02	49576	784
393	28.01	68730	928	332	26.02	83425	551
				504	26.02	90423	781
801	26.02	40989	236				
788	26.01	16369	29	771	28.01	53365	181
848	28.01	53365	174				
979	7.00	28839	965	974	7.00	28838	965
995	15.00	0	6	983	23.01	339	771
				45	26.02	63466	743
129	26.02	63425	752				
193	26.02	82382	950				
242	26.02	89907	846	242	26.02	89907	795
255	28.01	53365	98				

Figure 9 (Continued)

Figure 9 (Continued)

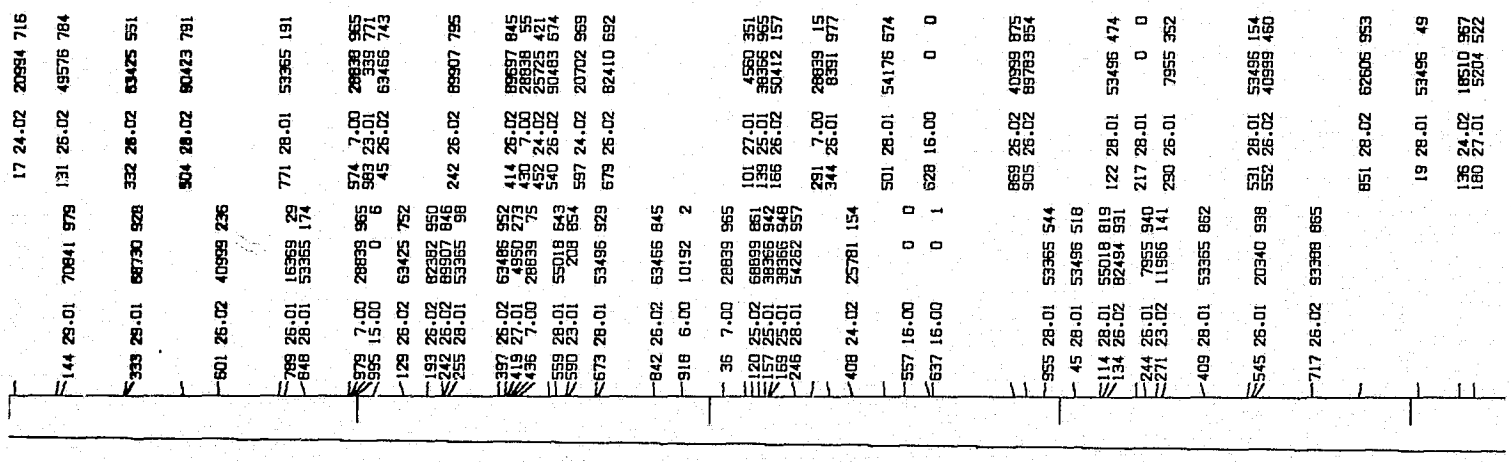

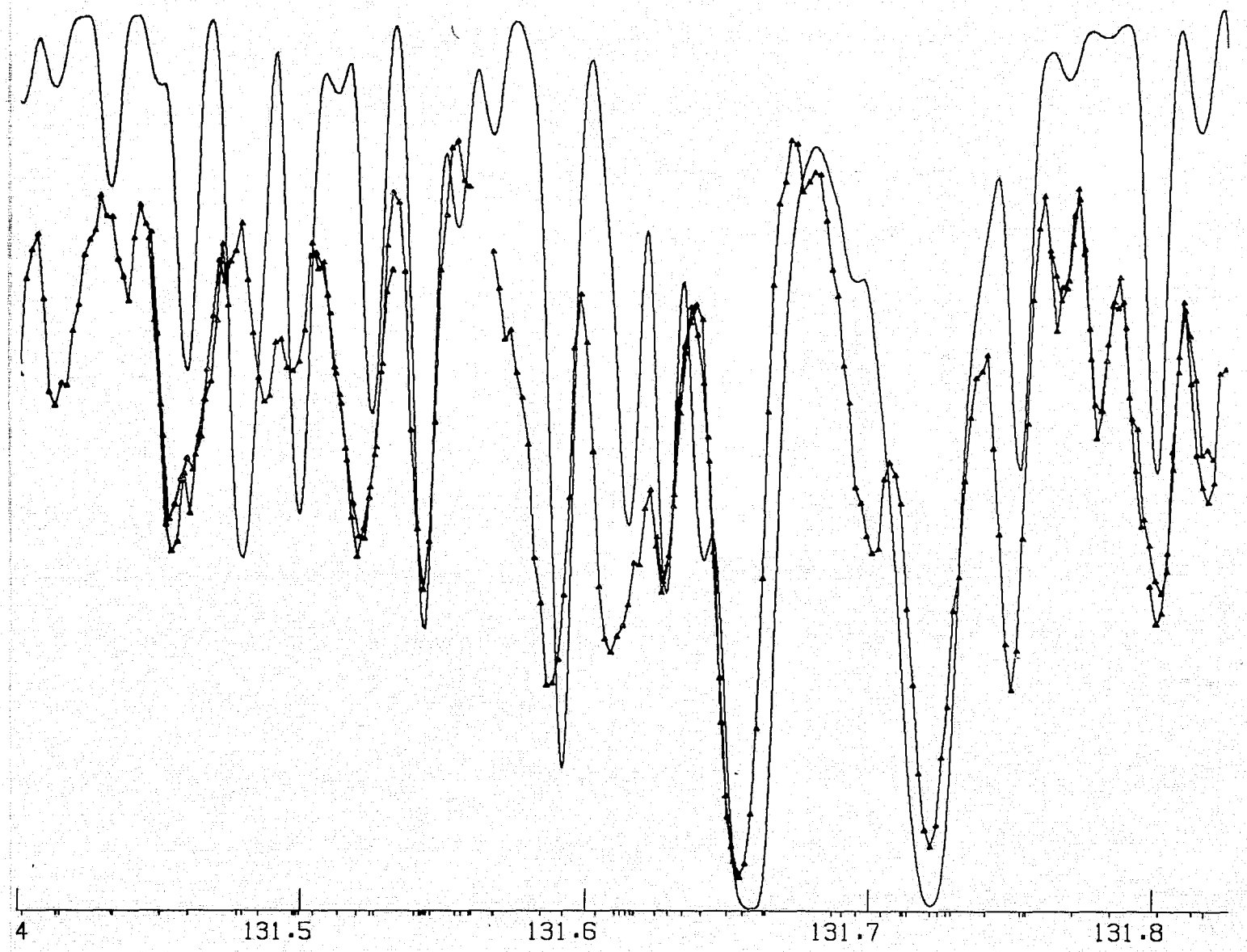

Figure 9 (Continued)

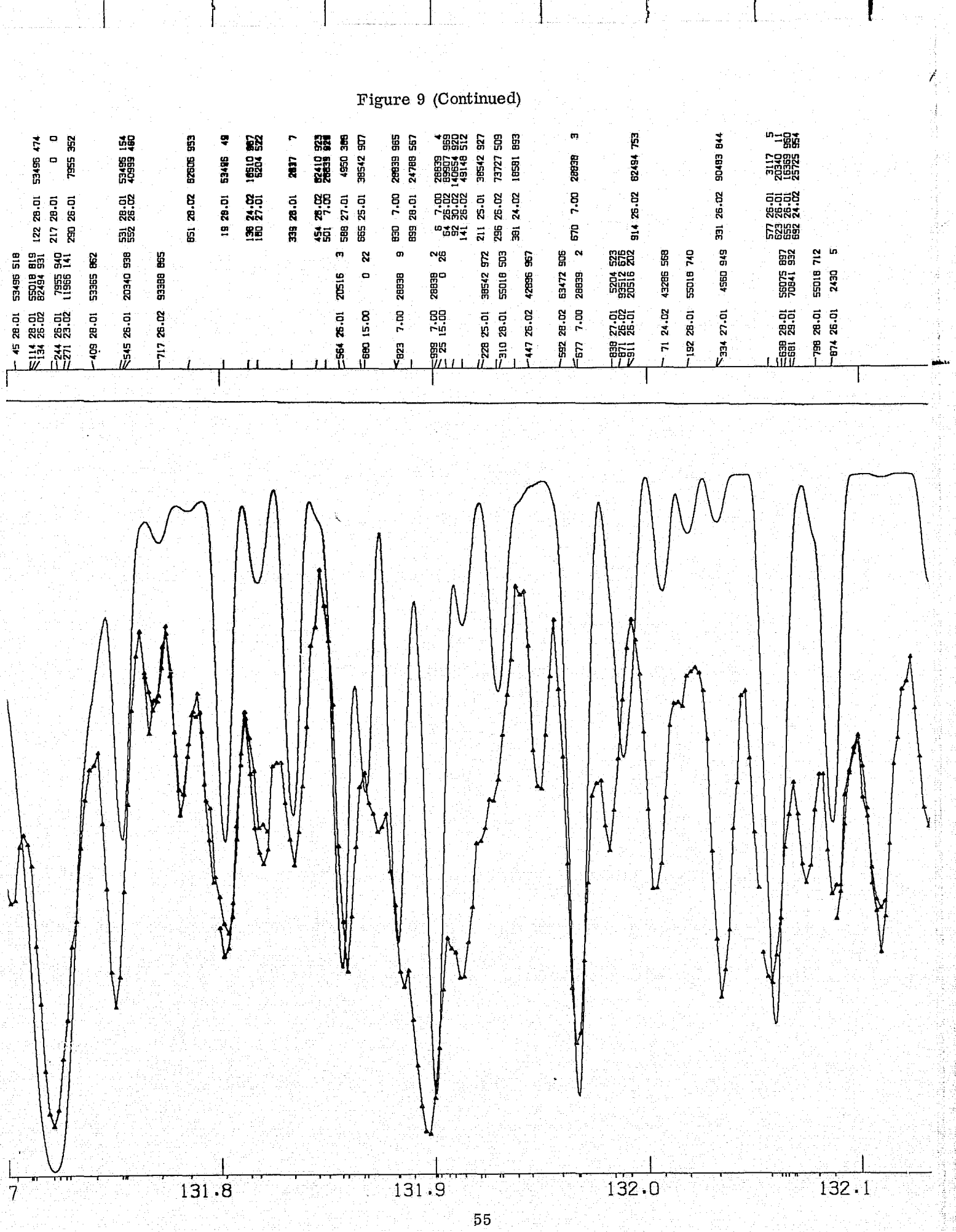

Figure 9 (Continued)

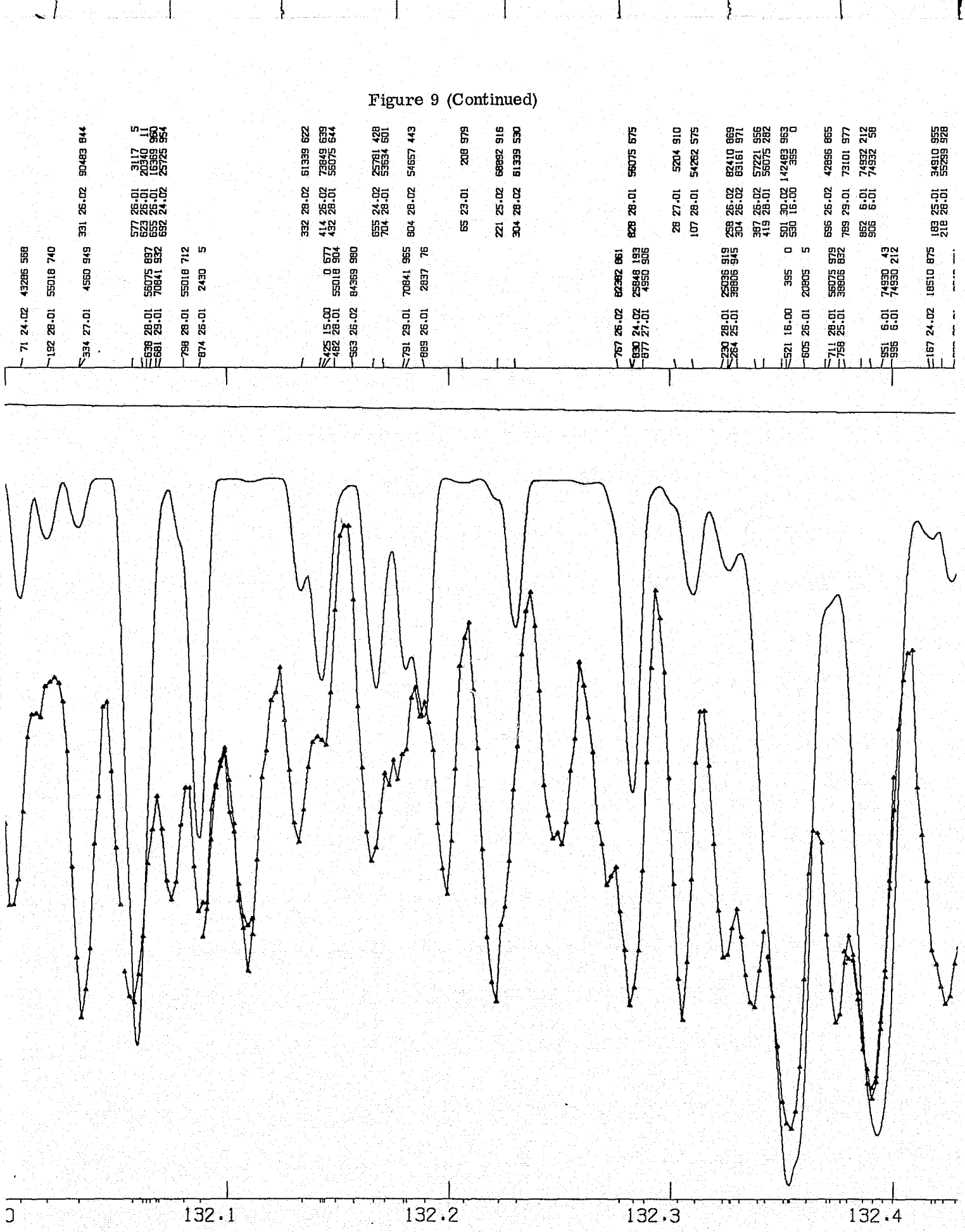

Figure 9 (Continued)

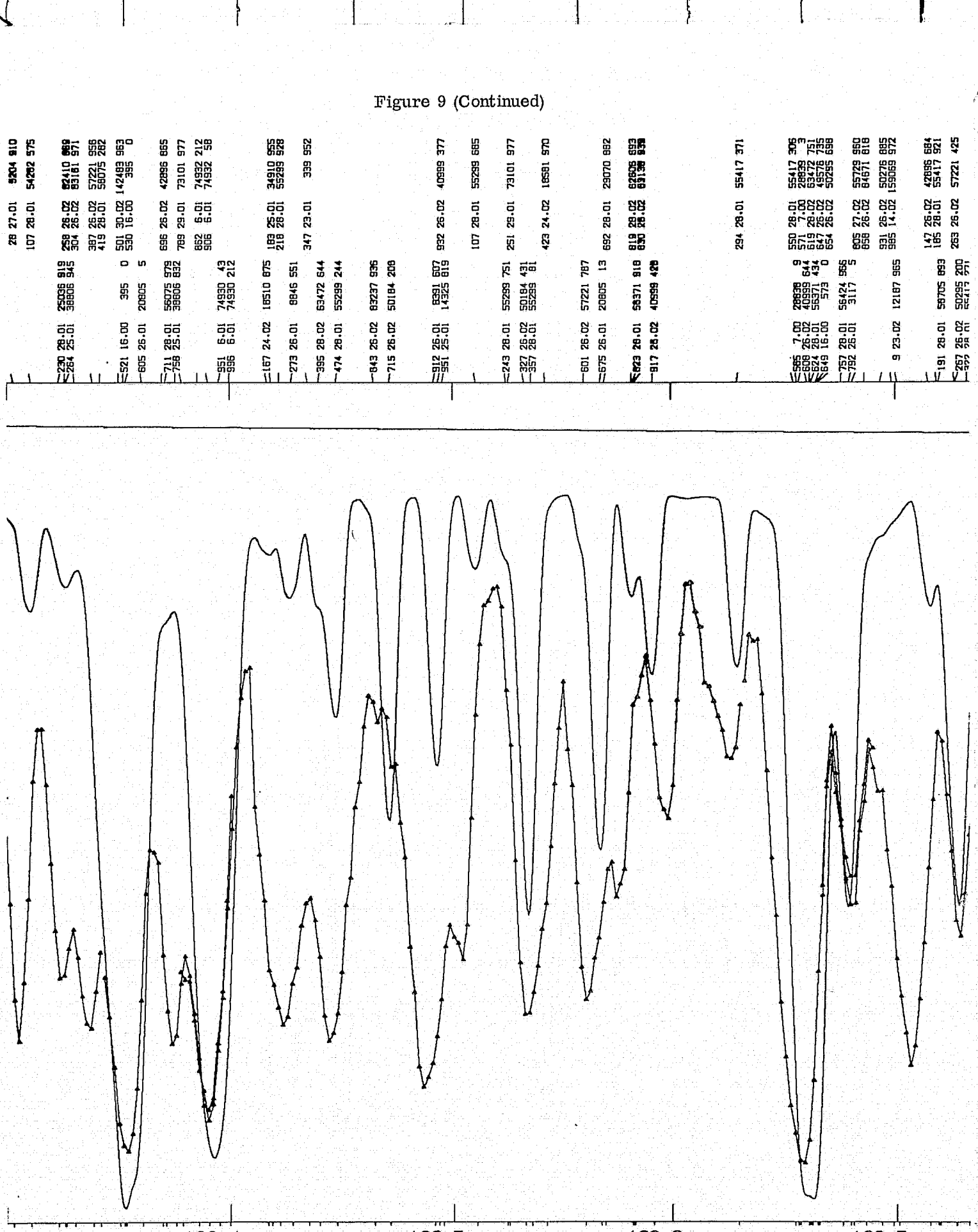

Figure 9 (Continued)

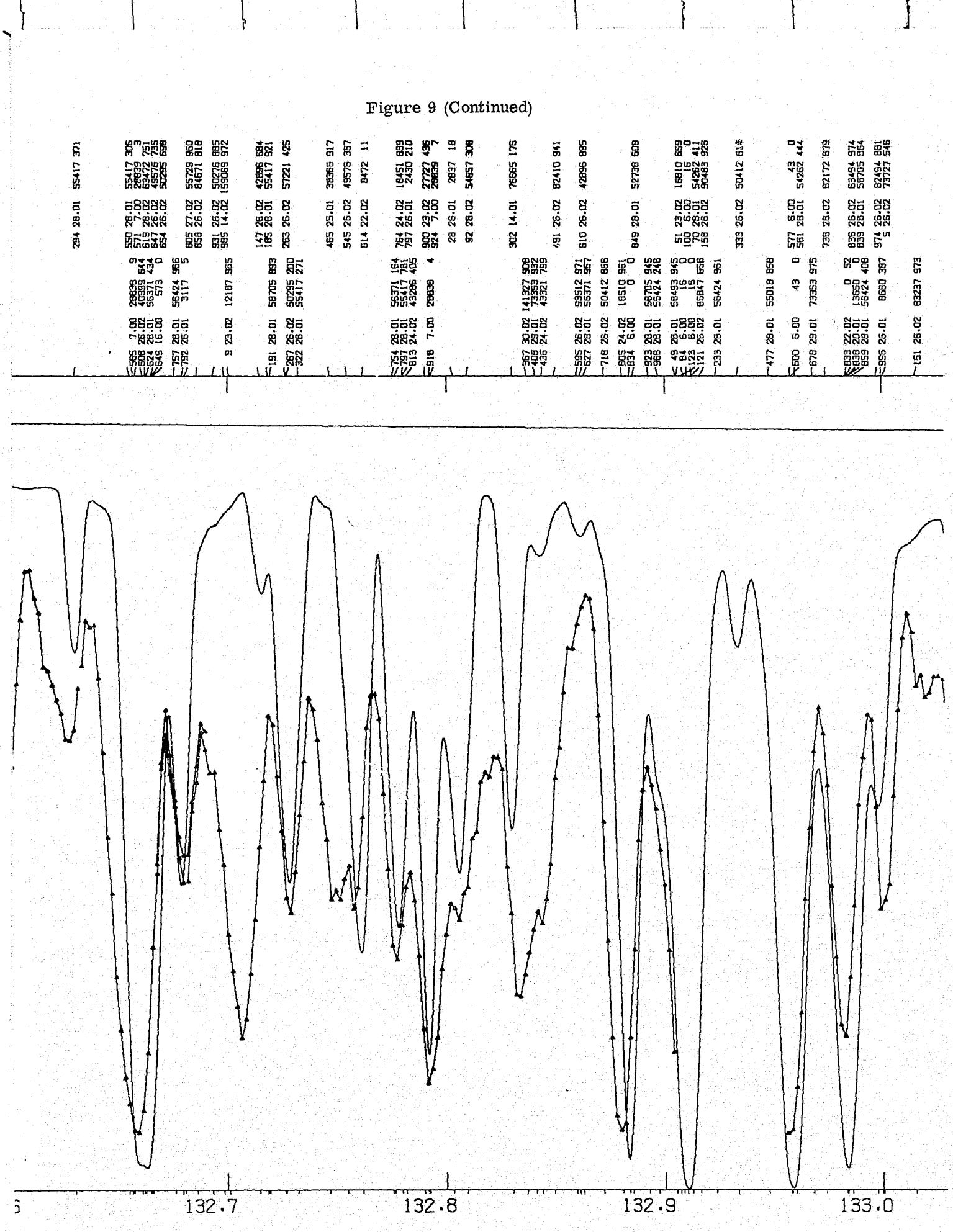

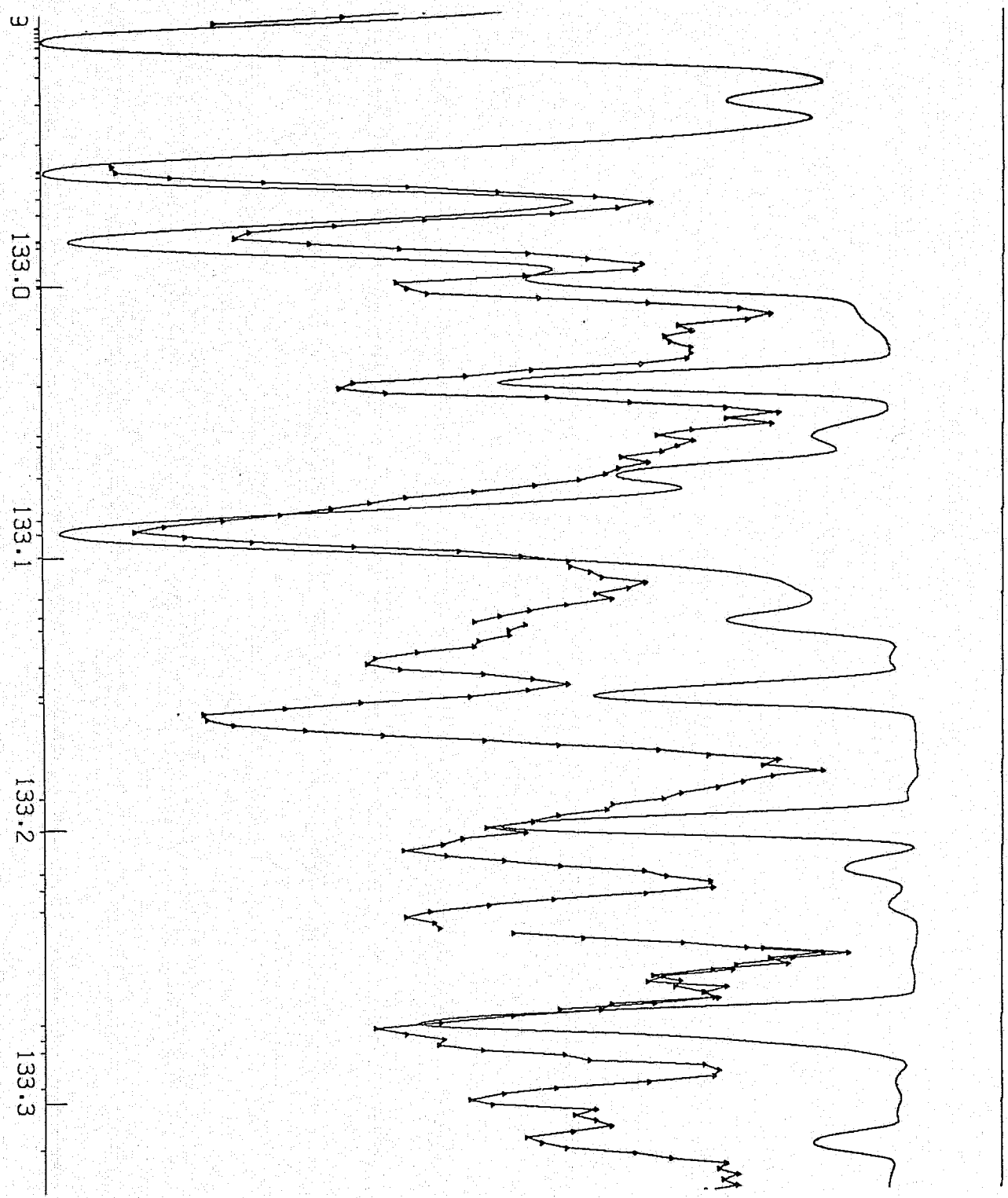

49 28.01 58493 945
84 6.00 16 0
123 6.00 16 0
121 26.02 86847 958
233 28.01 56424 961
477 28.01 55018 858
600 6.00 43 0
678 29.01 73353 975
833 22.02 0 52
838 20.01 13650 0
859 28.01 56424 408
996 26.01 8680 387
151 26.02 83237 973
363 26.02 50276 194
590 25.01 38542 889
912 20.01 13710 0
997 26.02 69836 976
884 29.01 71493 960
2 23.02 16977 101
157 26.02 73649 772
712 26.01 18360 8
766 23.02 12187 928

51 23.02 16810 859
100 6.00 16 0
70 28.01 54262 411
158 26.02 80483 826
333 26.02 50412 614
577 6.00 43 0
581 28.01 54262 444
738 28.02 82172 879
836 26.02 63494 974
839 28.01 58705 864
974 26.02 82494 881
5 26.02 73727 545
549 28.01 54262 822
701 26.02 50295 445
859 25.01 14325 975
912 20.01 13710 4
149 26.02 84369 903
218 24.02 43304 788
266 28.01 55018 560
506 25.01 14325 387
530 24.02 43321 441
216 29.01 71493 939
295 26.02 83358 901
767 28.01 54262 510
812 28.01 58705 790
945 28.01 54262 954
172 28.01 54262 678

Figure 9 (Continued)

Figure 9 (Continued)

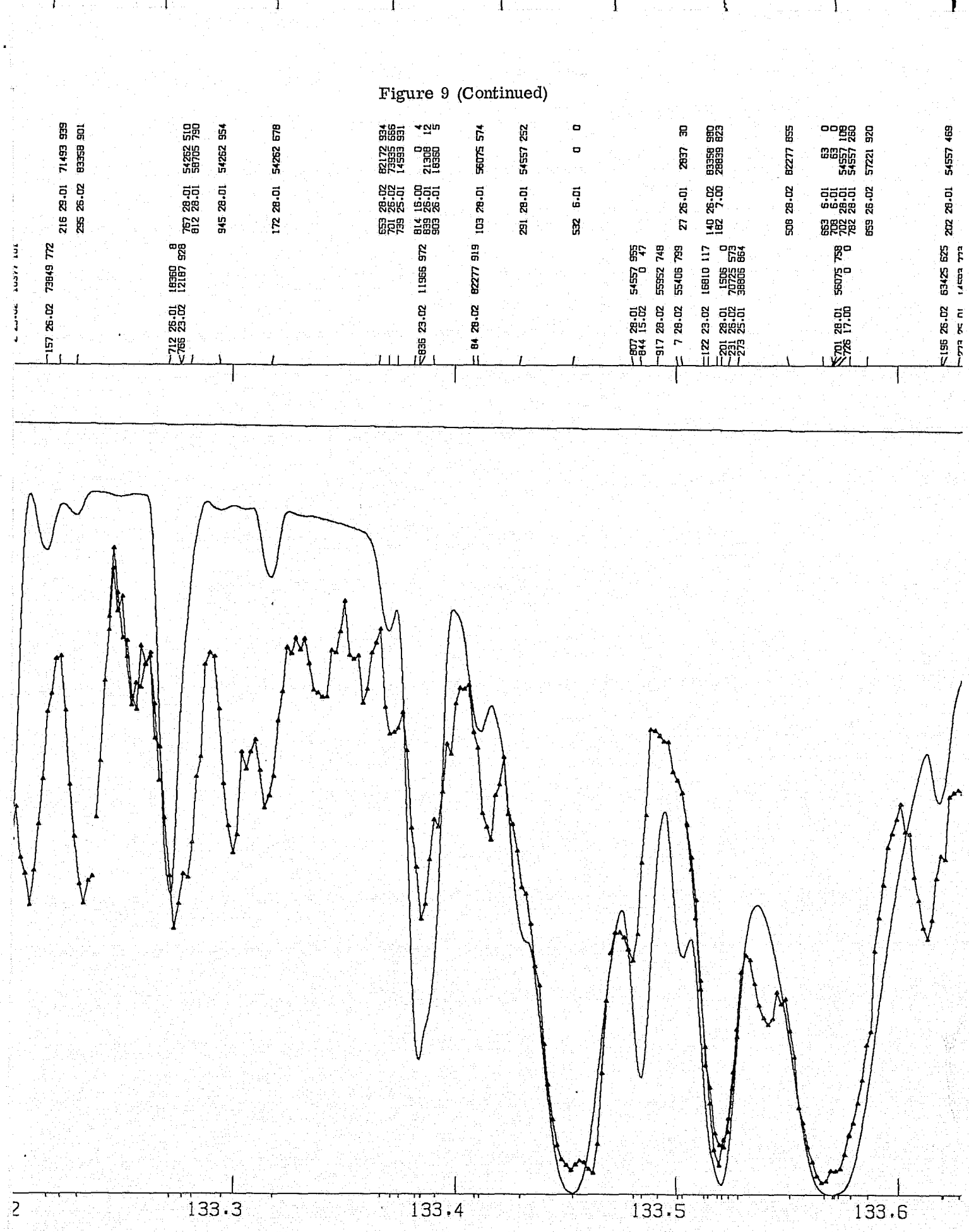

Figure 9 (Continued)

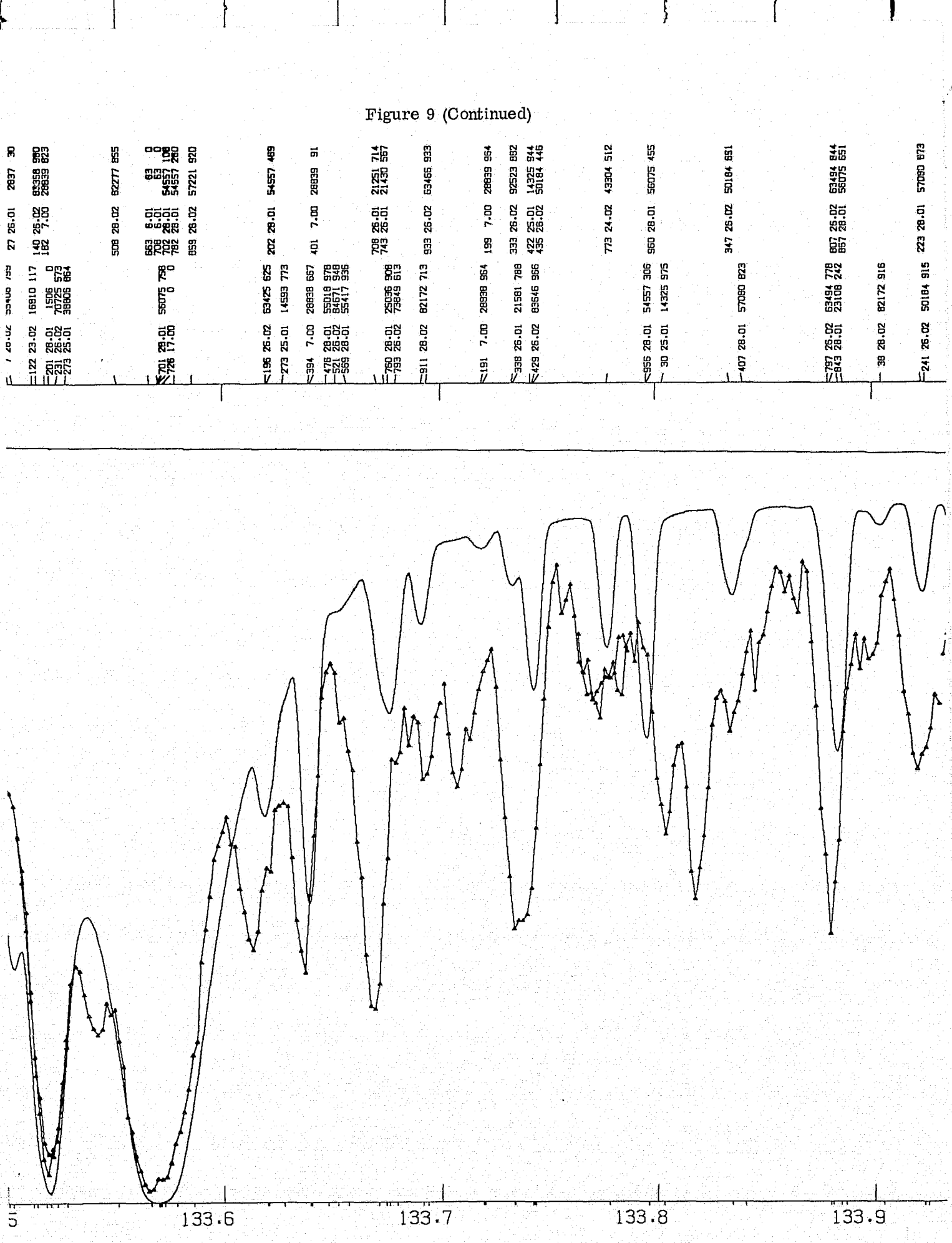

Figure 9 (Continued)

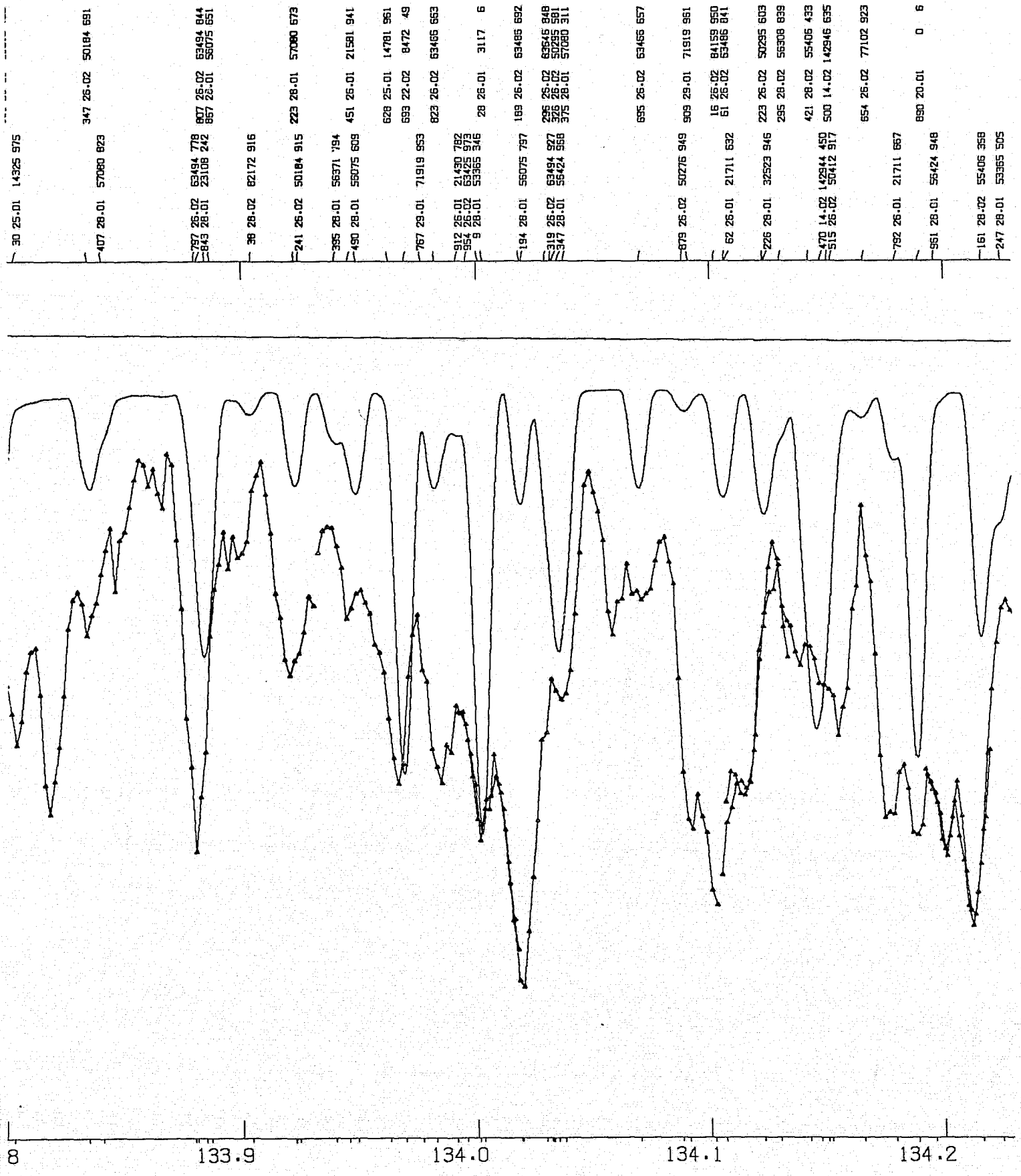

Figure 9 (Continued)

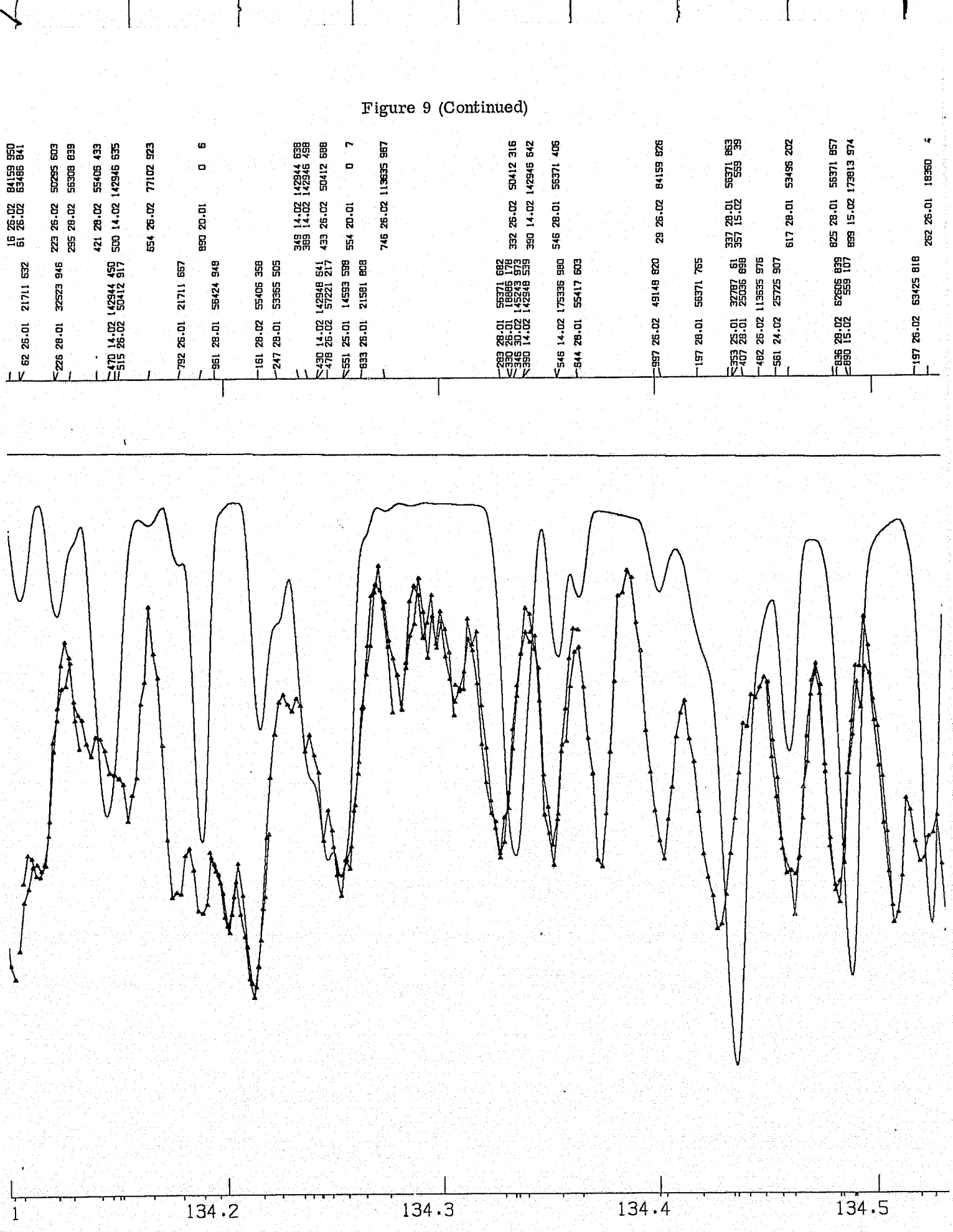

Figure 9 (Continued)

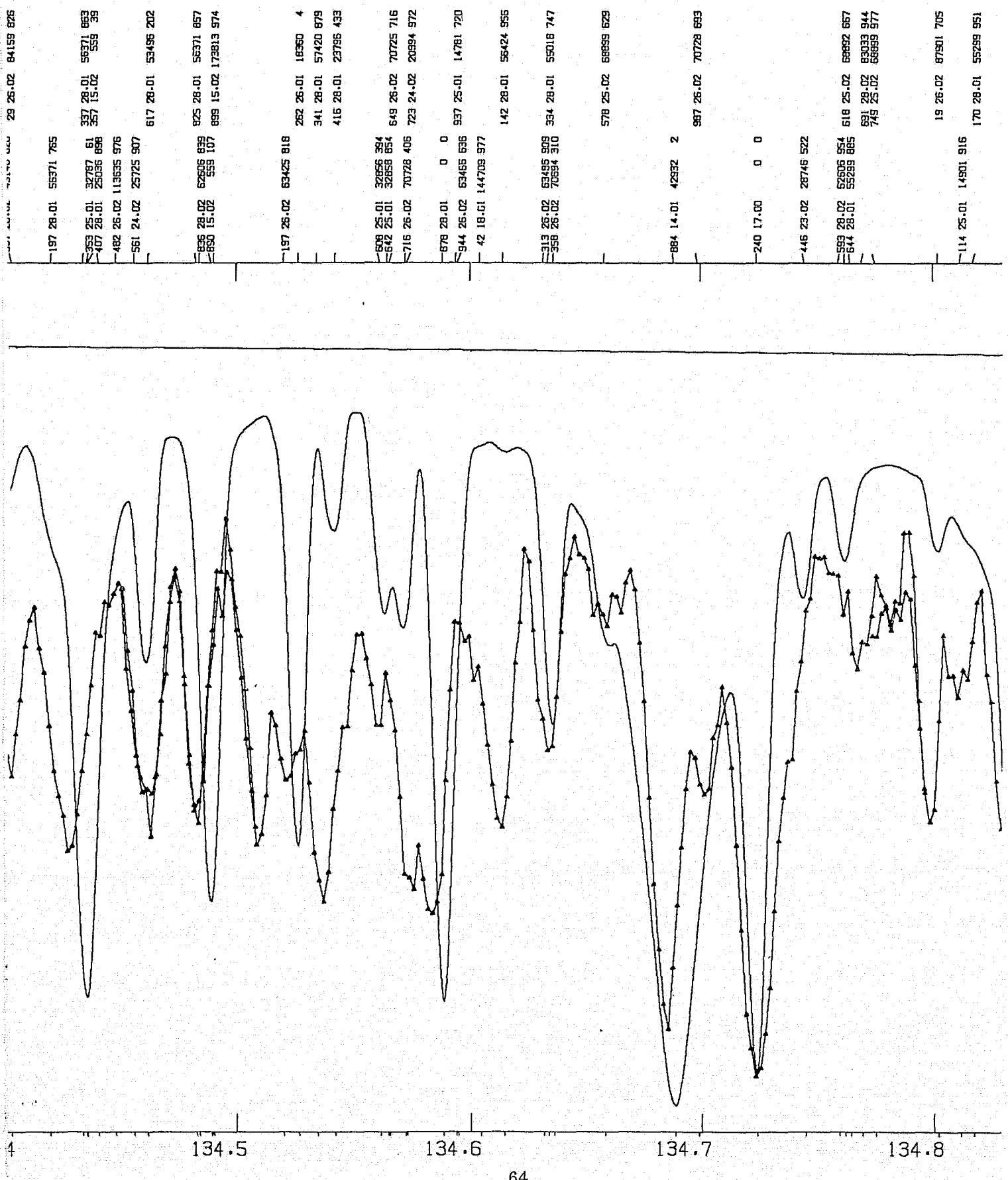

Figure 9 (Continued)